# Understanding the Interaction between LRRK2 and PINK1: Implications for Parkinson's Disease

by

**Salvatore James Cherra, III**

Bachelor of Science, The University of Scranton, 2006

Submitted to the Graduate Faculty of

the School of Medicine in partial fulfillment

of the requirements for the degree of

Doctor of Philosophy

University of Pittsburgh School of Medicine

2011

UNIVERSITY OF PITTSBURGH

SCHOOL OF MEDICINE

This dissertation was presented

by

Salvatore James Cherra, III

It was defended on

July 25, 2011

and approved by

Robert Bowser, PhD, Associate Professor, Department of Pathology

Billy W Day, PhD, Professor, Department of Pharmacology & Chemical Biology

Scott M Kulich, MD, PhD, Assistant Professor, Department of Pathology

Reza Zarnegar, PhD, Professor, Department of Pathology

Dissertation Advisor: Charleen T Chu, MD, PhD, Professor, Department of Pathology

**Understanding the Interaction between LRRK2 and PINK1: Implications for Parkinson's Disease**

Salvatore James Cherra, III, PhD

University of Pittsburgh School of Medicine, 2011

Parkinson's disease (PD) is a progressive neurodegenerative disorder that affects nearly 1% of the US population over the age of 65. While PD is primarily a sporadic disease, roughly 10% of PD cases are due to genetic mutations, giving rise to familial forms of PD. Interestingly, mutations in two kinases, the *leucine-rich repeat kinase 2 (LRRK2)* and the *PTEN-induced kinase 1 (PINK1)*, underlie two forms familial PD. Although the pathogenic mechanisms still remain unknown, many insights have been gained from investigating toxin insults and genetic mutations that cause parkinsonian phenotypes. Studies using neurotoxins and genetic mutations that underlie familial PD have implicated mitochondrial dysfunction in the pathogenesis of PD. This project sought to identify modes of neuroprotection that ameliorated the effects of LRRK2 mutations on neuronal and mitochondrial homeostasis. The mechanism of protein kinase A (PKA)-mediated neuroprotection was investigated in neurotoxin and genetic models of PD. This study also explored the mechanisms of PINK1-mediated neuroprotection. Activation of PKA prevented mutant LRRK2-induced neurite shortening by suppressing autophagy through the phosphorylation of the autophagy protein, the microtubule-associated protein light chain 3. This study also found that mutant LRRK2 causes mitochondrial degradation by autophagy in the dendrites of neurons, which led to shortening of the dendrites. PINK1 suppressed the autophagy induction elicited by mutant LRRK2 and prevented the mitochondrial degradation and neurite shortening. Furthermore, mutant LRRK2 caused a delay in calcium clearance after neuronal

depolarization. This prolonged elevation in intracellular calcium caused mitochondrial depolarization followed by degradation. Indeed, calcium chelation or inhibition of voltage-gated calcium channel restored calcium homeostasis and attenuated the mitochondrial degradation and dendrite shortening induced by *LRRK2* mutations. Finally using immunoprecipitation and 2-dimensional gel electrophoresis, PINK1 was found to interact with and regulate the phosphorylation status of proteins that maintain mitochondrial polarization, energy production, and calcium buffering. Overall, these results indicate that autophagy modulation and restoration of mitochondrial homeostasis protects against mutant LRRK2. This study proposes that calcium imbalance, mitochondrial dysfunction, and autophagy dysregulation are early events in the pathogenesis of familial and sporadic PD and thus, are potential therapeutic targets for PD.

## TABLE OF CONTENTS

## LIST OF TABLES

## LIST OF FIGURES

## ACKNOWLEDGMENTS

I would like to take this opportunity to thank all the people who have made this work possible. First, I would like to thank the other members of the Chu laboratory. You who have helped both inside and outside of the lab, I am greatly indebted. Without you this project could not be completed; you have helped me complete experiments, revise hypotheses, and decompress after failed experiments. To the members of the Chu lab, I will never forget you.

To the members of my dissertation committee, thank you for your time spent mentoring me, thank you for the critiques and criticisms that have made me a better scientist, and thank you for you wisdom and insights that I will take with me.

To my mentor, Charleen, first, thank you for letting me be a part of your lab. I appreciate you being there to discuss all aspects of life in science, from experimental ideas to career development and running a lab. You have provided me with the skills to succeed, and without you, I would not be the scientist I am today. Again, thank you.

To my friends and fellow graduate students, I greatly appreciate having you in my life. Whether it was rock climbing, kayaking, sporting events, or simply relaxing, you have made graduate school a complete experience. I am truly grateful to have met all of you and to have been fortunate enough to share my graduate school experience without.

To my family and friends, you have shaped my life the most. I can only hope that as I have grown throughput the years that I have made you proud. To my sister, parents, and

grandparents, I appreciate all of the support you have given throughout my life, whether it is a kind word, a listening ear, some much-needed advice, or thoughts on which to reflect. Thank you for fueling my inquisitive nature, for supporting my hopes and dreams, and for making me the person I am today. Without you, this would truly not be possible.

To my wife, Eva, words cannot describe how grateful I am to have someone with whom to share my highs, who carries me through my lows, and who enables me to do things I never thought were possible. I will never be able to express how thankful I am to have you. Like in the half marathons we run together, you have been my support when I couldn't go on alone, my rest when I am tired, and my sense of reason when I when I lose focus. When experiments fail and theories crumble, you remind me that life is full of things to appreciate even at times when graduate school seems impossible.

To everyone mentioned, thank you. I cannot even imagine what it would be like to try to accomplish this great feat without you.

## ABBREVIATIONS

ADT2 - adenine nucleotide transporter 2

Atg - autophagy-related gene

ATP - adenosine triphosphate

BAPTA-AM - 1,2-Bis(2-aminophenoxy) ethane-N,N,N′,N′-tetraacetic acid tetrakis (acetoxymethyl ester)

cAMP - cyclic AMP

Drp1 - dynamin-related protein 1

EGTA - ethylene glycol tetraacetic acid

GFP - green fluorescent protein

H89 - N-[2-(p-Bromocinnamylamino)ethyl]-5-isoquinolinesulfonamide dihydrochloride

LC3 - microtubule-associated protein 1B light chain 3

LRRK2 - leucine-rich repeat kinase 2

MAP2 - microtubule-associated protein 2

MAPK - mitogen-activated kinase

MPP+ - 1-methyl-4-phenylpyridinium

MPTP - 1-methyl-4-phenyl-1, 2, 3, 6-tetrahydropyridine

mTOR - mammalian target of rapamycin

PBS - phosphate buffered saline

PD - Parkinson's disease

PI3K - phosphatidylinositol-3 kinase

PINK1 - PTEN-induced kinase 1

PKA - protein kinase A

RNAi - RNA interference

ROS - reactive oxygen species

SDS-PAGE - sodium dodecyl sulfate polyacrylamide gel electrophoresis

shRNA - short hairpin RNA

TMRM - tetramethylrhodamine methyl ester

TRAP1 - TNF receptor-associated protein 1

VDAC - voltage dependent anion channel

# 1.0 INTRODUCTION

## 1.1 PARKINSON'S DISEASE

James Parkinson first described Parkinson's disease (PD) in his "An Essay on the Shaking Palsy" in 1817[1]. Currently, 1% of the US population above the age of 50 has been diagnosed with PD[2]. It is the second most common neurodegenerative disease, but the most common movement disorder. The cardinal symptoms of PD are thought to arise from deficits in the brain regions that control movement; these symptoms include bradykinesia (slowness of movement) or akinesia (lack of movement), resting tremor, muscle stiffness, and postural instability[3]. While the cause of disease remains poorly understood, the pathological hallmark is the degeneration of dopaminergic neurons in the midbrain. These midbrain dopaminergic neurons project from the substantia nigra pars compacta to the caudate and putamen and regulate the corticothalamic circuits involved in movement control[4]. Reduction in dopaminergic neurotransmission or degeneration of the dopaminergic neurons is proposed to underlie disease onset and progression[4].

There is currently no cure or treatment to slow the disease progression[5]. Levodopa, a dopamine precursor, is the most efficacious treatment for the disease; however, it only alleviates the symptoms of PD[5]. While other therapies that attempt to modulate dopamine levels or to prevent, repair, or replace the injured/lost dopaminergic neurons are under development, none have proved successful[5]. Although loss of the neurons in the substantia nigra pars compacta is

the key pathological finding indicative of PD, there is evidence that other brain regions are affected[6]. For example, aberrations in the olfactory system and difficulty sleeping have been reported in patients, as well as the occurrence of dementia and other cognitive defects[3]. These findings suggest that PD may have more widespread effects on the brain outside of the basal ganglia, which could explain why previous therapies focused on the midbrain dopamine system have lacked efficacy.

In order to more fully understand the disease process, studies have combined observations acquired from human tissue samples and animal and cell culture systems utilizing neurotoxin and genetic models of PD. Data gathered from these studies suggest that pathways that regulate mitochondrial homeostasis, intracellular calcium handling, and protein degradation may provide points of convergence between various models of PD and patient samples[7-9].

### 1.1.1 Mitochondrial Homeostasis

Mitochondria, frequently referred to as the powerhouse of the cell, produce energy and biosynthetic molecules, serve as a calcium buffer, and regulate apoptotic and necrotic cell death[10]. Through the use of the glucose metabolite, pyruvate, mitochondria produce ATP using the electron transport chain to satisfy most of the cell's energy requirements. The production of ATP relies on the proton electrochemical gradient established across the mitochondria inner membrane; as protons flow down their gradient into the matrix, the mitochondria utilize this energy to drive ATP synthesis[10]. This ATP production fuels many cellular processes, including proliferation, differentiation, many homeostasis events, and the suppression of cell death.

Calcium homeostasis is maintained through a network of calcium channels and calcium binding proteins that prevent intracellular calcium overload[8]. Calcium enters neurons through n-

methyl-d-aspartate receptors and voltage-gated calcium channels during neuronal depolarization[8]. Intracellular calcium is then either extruded through the plasma membrane calcium ATPase or sequestered within the endoplasmic reticulum via the sarco/endoplasmic reticulum calcium ATPase[8]. The mitochondria serve as an additional reservoir during periods of elevated intracellular calcium[11]. Calcium is transported into the mitochondria, in part, through the voltage-dependent anion channel (VDAC) and the mitochondrial calcium uniporter[12, 13]. Upon entry, calcium flows into the negatively charged matrix, where it forms calcium-phosphate complexes that precipitate under high levels (0.2-2μM) of calcium, allowing the mitochondria to provide calcium buffering independent of the matrix calcium concentration[11]. The uptake of calcium slightly diminishes the electrochemical gradient, which is observed as a reduction in mitochondrial polarization using the mitochondrial membrane potential-dependent dye, TMRM[11, 14]. After the intracellular calcium loading has subsided, mitochondria gradually release calcium into the cytoplasm for extrusion to return to basal intracellular calcium levels[11].

Under extreme cases, the mitochondria can actually become completely depolarized, a process known as the mitochondrial permeability transition[11]. The formation of the mitochondria permeability transition pore allows for the release of proteins and ions from mitochondria, such as cytochrome c and calcium, which leads to apoptotic cell death[15]. This pore is comprised of VDAC, the adenine nucleotide transporter (ADT), and cyclophilin D[15]. Inhibition of this complex through small molecules or genetic manipulations prevents apoptotic cell death and increases the calcium buffering capacity of mitochondria[11]. Once the electrochemical gradient is depleted, mitochondria cease to respire, leading to the reduction/termination of ATP production, which has been associated with the induction of necrotic cell death[15]. With its roles in ATP

production and calcium buffering, the mitochondria also regulate the execution of cell death via apoptosis or necrosis.

Due to the high requirement of mitochondrial function for neuronal homeostasis, it is no surprise that conditions that reduce mitochondrial function ultimately lead to disease. While the entire body is subjected to environmental or genetic stresses that could give rise to PD, the substantia nigra is particularly sensitive to mitochondrial stress. Dopaminergic neurons in the substantia nigra contain fewer mitochondria than surrounding brain regions[16]. This suggests that mitochondrial dysfunction would greatly impact these neurons, which possess a smaller network of mitochondria. These neurons also display a reduced calcium buffering capacity[17]. Together, the reduced mitochondrial content and the low calcium buffering capacity would make these cells susceptible to calcium-induced injury from the tonic calcium waves that establish the rhythmic firing patterns of substantia nigra dopaminergic neurons. One study found that substantia nigra neurons expressing high levels of the calcium binding protein, calbindin, were spared in PD patients, suggesting that enhanced calcium buffering may provide protection from disease[18]. Both the reduced calcium buffering and low mitochondrial content combined with mitochondrial toxin and genetic stresses implicate the loss of mitochondrial homeostasis or increased mitochondrial dysfunction as key events in PD pathogenesis.

### 1.1.2 The Kinases of Parkinson's Disease

The genes associated with familial forms of PD encode a variety of different proteins. Interestingly, two genes *PINK1* and *LRRK2* encode the kinases: the PTEN-induced kinase 1 and the leucine-rich repeat kinase 2, respectively. PINK1 is a 581 amino acid protein that contains a mitochondrial targeting sequence, a transmembrane domain, and a kinase domain[19]. Mutations in

*PINK1* have been associated with an autosomal recessive, early-onset form of PD[20-23]. Due to the recessive nature of familial PD associated with *PINK1*, the mutations arising in *PINK1* are thought to produce loss of function mutants[24]. Indeed, loss of PINK1 results in mitochondrial aberrations, elevated production of reactive oxygen species, increased numbers of autophagosomes, decreased calcium buffering, and cell death in tissue culture[25-30]. Reduced kinase activity in a number of disease-associated mutants further supports this loss of function phenotype[24]. Although PINK1 deficiency in tissue culture recapitulates many of the findings reported in PD or toxin models, *PINK1*$^{-/-}$ animals fail to show neurodegeneration or behavioral deficits indicative of PD[27, 31]. This discrepancy between tissue culture and animal models may suggest modes of compensation or that lack of PINK1 does not fully reflect the dysfunction of PINK1 mutants.

While disease-associated mutations in *PINK1* were identified 7 years ago, the function of PINK1 and its substrates remain unknown[22]. Pridgeon and colleagues have identified TRAP1 as a potential PINK1 substrate; however, the biological function of this phosphorylation has yet to be determined[32]. In addition, to its interaction with the TNF receptor-associated protein 1 (TRAP1), PINK1 has been shown to bind to other chaperones and Milton and Miro, which regulate mitochondrial trafficking[33]. Even though little is known about PINK1 signaling pathways, one robust finding is that overexpression of wild type PINK1 provides protection against a number of neurotoxic insults[25, 32, 34]. These protective effects have been attributed to its reduction in cytochrome c release and its role in maintaining mitochondrial homeostasis by regulating reactive oxygen species production, mitochondrial function, and mitochondrial degradation[25-30, 32, 34, 35]. The effects of PINK1 deficiency and PINK1 overexpression support the hypothesis that mitochondrial dysfunction plays a role in PD.

Previously RNAi against *PINK1* has been shown to elicit an increase in mitochondrial localized ROS production and mitochondrial fragmentation[25]. While inhibition of mitochondrial fission via expression of a dominant negative Drp1 suppressed fragmentation, it did not reduce mitochondrial ROS production[25]. Interestingly, antioxidants suppressed both ROS production and mitochondrial fragmentation, indicating that ROS production is upstream of mitochondrial fragmentation and the cell death that follows[36]. Mitochondrial dysfunction caused by RNAi against PINK1 also induces autophagy, which restores mitochondrial homeostasis by degrading damaged mitochondria[25]. Inhibition of canonical autophagy via RNAi against beclin-1 or PI3K inhibitors exacerbated cell death caused by PINK1 deficiency[25], supporting its prosurvival role in this model. This previous study also showed that PINK1 overexpression suppressed autophagy induced by the neurotoxin, 6-hydroxydopamine, suggesting that PINK1 levels regulate autophagy through an unknown mechanism[25].

Mutations in *LRRK2*, however, cause an autosomal dominant form of PD, and therefore, the mutations are thought to be gain of function mutations[37, 38]. *LRRK2* encodes a multidomain protein that includes leucine-rich repeats, a kinase domain, a GTPase domain, an ankyrin domain, and a WD40 domain. Surprisingly, disease-associated mutants have not been linked to a single domain, but rather pathogenic mutations have been identified in each domain[37, 38]. Although some mutants are more penetrant or produce more severe phenotypes, the fact that mutations in any domain can cause disease suggests that LRRK2 plays a complex, multifaceted role in regulating neurobiology.

Although the precise functions of LRRK2 are poorly understood, mutations perturb membrane trafficking pathways[39-41], cytoskeletal dynamics[42-44], and protein translation[45, 46]. Mutant LRRK2 elicits an increase in autophagy as well as aberrations in endocytosis[39-41]. In

neurons, there are also defects in synaptic vesicle trafficking[47, 48]. Since all of these events require microtubule networks, it is interesting to note that mutant LRRK2 also reduces microtubule dynamics through the direct phosphorylation of tubulin[42]. This would lead to more stabilized networks that are less capable of rearranging to provide new routes for protein and organelle trafficking, which would be required for development, plasticity, and cellular maintenance. LRRK2 also phosphorylates 4E-BP, which regulates protein synthesis[46]. Together these findings suggest that LRRK2 could affect neuronal maintenance through its effects on biosynthesis and trafficking of proteins and organelles.

A previous study found that expression of mutant LRRK2 elicits an increase in autophagosomes and a decrease in neurite length[41]. Inhibition of autophagy prevented the neurite shortening induced by mutant LRRK2, whereas autophagy induction with rapamycin exacerbated the neurite shortening[41]. Interestingly, PI3K inhibitors, which inhibit canonical autophagy, did not suppress the mutant LRRK2 induced autophagy[41]. However, inhibition of the MAPK signaling pathway using a MEK inhibitor reduced the number of autophagosomes and provided protection against neurite shortening[41]. This study indicates that mutant LRRK2 elicits a non-canonical autophagy-mediated neurite retraction.

## 1.2 AUTOPHAGY

Neuronal maintenance and mitochondrial homeostasis are two overarching themes for PD that are regulated by biosynthetic and degradation pathways. Autophagy is a highly orchestrated intracellular degradation pathway through which cytoplasmic components are trafficked to the lysosome for degradation[49]. Sam Clark, Jr. first discovered this highly conserved pathway in

1957 during normal kidney development[50]. Since its initial discovery, various forms of autophagy have been observed in all eukaryotic model organisms including: yeast, worms, flies, rodents, plants, and humans[49]. Such strong conservation highlights the importance of this pathway to the health and survival of living organisms.

Originally identified as a survival pathway utilized during times of nutrient starvation, the autophagy pathway has been implicated in a multitude of new roles due to immense growth in the research field. Similar to its function for overcoming times of nutrient deprivation, it is not surprising that multiple studies have implicated the autophagy pathway in longevity and healthy aging[51]. In addition to its widespread roles across the eukaryotic domain, it is no surprise that a function for autophagy pathway has been observed in all human tissue systems. Based on these findings, researchers began to investigate the effects of the autophagy pathway in human disease. To date, the autophagy pathway has been implicated in either a pathogenic or protective role in a number of neurodegenerative diseases[52], cardiovascular disease[53], Crohn's and other gastrointestinal diseases[54], innate and adaptive immunity[55], and many forms of cancer[56]. Not only has autophagy been thoroughly observed in multiple roles of cellular homeostasis, but different types of autophagy have also been identified and characterized.

### 1.2.1 Types of Autophagy

There are currently three types of autophagy: microautophagy, chaperone-mediated autophagy, and macroautophagy. Microautophagy occurs when proteins or other cytoplasmic constituents are engulfed by lysosomal invagination[52]. This provides a single, direct step for protein degradation by the lysosome.

Chaperone-mediated autophagy denotes the process whereby chaperones recognize and deliver proteins targeted for degradation to the lysosome[57]. The cargo interacts with lysosomal receptors, which facilitate its entry into lysosomes[57]. Unlike micro- and macroautophagy, chaperone mediated autophagy is saturable due to its reliance on lysosomal receptors for protein entry into the lysosome. While these autophagy pathways are experimentally separable and differentially regulated, macroautophagy is capable of compensating for deficits in or saturation of chaperone-mediated autophagy[58].

Macroautophagy, which henceforth will be referred to as autophagy, is the process where cytoplasmic components are sequestered by double membrane-bound vesicles called autophagosomes. Once engulfed, the cargo is trafficked along microtubules to the lysosome, where the lumenal contents are degraded. In mammalian cells, the autophagy pathway can be separated into four steps: (1) initiation of phagophore formation, (2) sequestration of cargo within the autophagosome, (3) delivery of cargo to the lysosome, and (4) degradation of cargo and efflux of macromolecules[59].

### 1.2.2 The Canonical Autophagy Pathway

Initiation is accomplished by upstream stress response and signaling pathways, which integrate cellular information and activate autophagy-executing proteins. Canonical autophagy induction is regulated by the mammalian target of rapamycin (mTOR)[59]. Under nutrient rich conditions, mTOR suppresses autophagy induction and increases protein translation[59]. During nutrient starvation, however, mTOR is inhibited and autophagy is induced as a means to produce energy. The inhibition of mTOR leads indirectly to the dephosphorylation of Atg13, which in its dephosphorylated state interacts with Atg1[59]. This Atg13-Atg1 complex then signals through an

unknown mechanism to induce autophagosome formation. In addition to the mTOR-Atg1-Atg13 signaling network, nutrient starvation also activates a class III phosphatidylinositol-3-kinase (PI3K)/beclin-1 complex[59]. The PI3K leads to increased phosphatidylinositol phosphorylation, which demarcates membranes for autophagosome formation[60].

Once initiated, the signal to induce autophagy is transduced to the core autophagy-executing proteins, which include Atg3, 4, 5, 7, 8, 9, 10, 12, and 16L. To create an autophagosome, Atg9, the only transmembrane protein in the core machinery, localizes to phagophore-forming structures[61]. Atg12 is conjugated to Atg5 through a ubiquitin-like reaction via Atg 7 and 10[62]. The Atg5-12 conjugate interacts with Atg16L and translocates to Atg9-positive structures. The membrane-associated Atg5-12-16L complex has been hypothesized to act as the E3-like enzyme in the lipid conjugation of LC3.

Prior to its lipidation, LC3, a 147 amino acid protein, is cleaved by Atg4 at glycine-120[62]. This exposed glycine is then conjugated to a lipid moiety, most commonly phosphoethanolamine[62]. This lipidation of LC3 is catalyzed by another ubiquitin-like conjugation system, in which Atg3 and 7 acts like E1 and E2 ubiquitin ligases, respectively[62]. Once attached to the phagophore, LC3 regulates the extension, curvature, and closure of the membrane[63]. It also acts as a receptor for cargo via adapter proteins, including p62/sequestrasome 1 and NBR1[64, 65]. Atg4 removes LC3 from the cytoplasmic surface when the autophagosome is complete[62].

Upon closure of the autophagosome, it traffics along microtubules to fuse with the lysosome[49]. Lysosomal acidification is necessary for fusion with the autophagosome based on the findings that bafilomycin A, a lysosomal ATPase inhibitor that prevents acidification, inhibits fusion[66]. Once fused, the autolysosome utilizes acid hydrolases, peptidases, and

proteases to digest the lumenal components from the autophagosome, as well as cargo-recognition proteins and any LC3 on the inner membrane. Autophagic degradation is completed with the release of macromolecules into the cytoplasm through Atg22, the lysosomal effluxer[52].

### 1.2.3 Autophagy in the Nervous System

Over the last few decades, the roles of autophagy in the nervous system have been under heavy investigation. Most of this work has been fueled by one of the pathological observations from many neurodegenerative diseases: protein aggregates. Amyotrophic lateral sclerosis, Alzheimer's, Huntington's, and Parkinson's disease all have protein aggregates as pathological hallmarks[59]. Early research focused on the identification and use of autophagy inducers to degrade these aggregates. However, recent evidence suggests that excessive induction of autophagy has deleterious effects in the nervous system[52, 59]. Instead, a balance between autophagy induction and lysosomal degradation has been hypothesized to be a more beneficial therapeutic target[52, 59].

While excessive autophagy may be detrimental, deficiencies in autophagy in the nervous system are sufficient to cause neurodegeneration. One example is the knockout of Atg5 or Atg7 under the nestin promoter[67, 68]. Both knockout mice show overt signs of neurodegeneration, including aggregates containing ubiquitinated proteins, neuronal cell loss, and behavioral abnormalities[67, 68]. In addition to experimental knockout of autophagy genes, a decrease in beclin-1, a protein involved in autophagy induction, has been observed in aged human subjects and Alzheimer's disease patients[69, 70]. Moreover, deficits in autophagy maturation or lysosomal degradation have been described in lysosomal storage diseases and Alzheimer's disease[71-73].

Together these data indicate that deficits in autophagy may underlie certain neurodegenerative diseases.

As previously mentioned, overactivation of autophagy could be as harmful as defects in autophagy. Mutations in LRRK2 or treatment with the neurotoxin, MPP+, elicit neuronal injury that requires autophagy induction[40, 41, 74]. In these models, autophagy inhibition is protective. One interesting observation from these studies is that autophagy induction in these situations is independent from PI3K regulation[41, 74]. Similar observations have also been made in non-neuronal cells, indicating the existence of a non-canonical autophagy pathway that is activated under pathological conditions. Therefore, therapeutic targeting of the autophagy pathway has proven more a tenuous task. Rather than simply inducing or inhibiting autophagy based on disease states, it is important to determine the underlying reasons for the protein aggregates or autophagy induction, since models for the same disease often contradict each other in terms of autophagy regulation.

## 1.3 PKA SIGNALING AND NEUROPROTECTION

Activation of the protein kinase A signaling pathways possesses neuroprotective effects against PD neurotoxins[75, 76]. Protein kinase A (PKA) regulates many intracellular signaling pathways that regulate proliferation, differentiation, cellular homeostasis, and cell death. PKA is a holoenzyme comprised of two regulatory subunits and catalytic subunits[77]. Upon binding of cAMP to the regulatory subunits, the catalytic subunits are released to phosphorylate downstream targets[77]. The activity of PKA is regulated upstream by adenylyl cyclase, which catalyzes the production of cAMP from ATP, and a phosphodiesterase, which converts cAMP

into AMP. In addition to regulation of its activity, PKA is regulated by its localization, which is maintained via interactions between the regulatory subunits and A-kinase anchoring proteins (AKAPs)[77]. Previous studies have identified AKAP scaffolds linking PKA to microtubules, mitochondria, the endoplasmic reticulum, the nucleus, and synapses[78]. AKAP also binds to some downstream signaling molecules and regulators of PKA, thus providing a highly localized signaling complex[78].

In neurons, PKA has been shown to regulate neurite outgrowth and synaptic plasticity through transcriptional (e.g. the cAMP response element binding protein (CREB)-mediated) and post-translational mechanisms, such as phosphorylation of α-amino-3-hydroxy-5-methyl-4-isoxazolepropionic acid receptors[79, 80]. Under pathological conditions, PKA provides protection from a numerous toxin insults, including the PD neurotoxin, 6-hydroxydopamine[75]. In addition to its anti-apoptotic effects and neurotrophic factor secretion, PKA increases mitochondrial function and suppresses autophagy in non-neuronal cells[81-83]. Overall, these studies suggest that PKA regulates many pathways, whose manipulation could provide therapeutic benefits for PD and other neurodegenerative diseases.

# 2.0 RATIONALE AND HYPOTHESES

Proper mitochondrial function is essential for neuronal function, and mitochondrial dysfunction has been widely associated with neurodegenerative diseases, including PD. I hypothesize that mutations in LRRK2, which cause familial PD, will affect mitochondrial homeostasis. Autophagy has been previously shown to play an integral role in maintaining mitochondrial homeostasis. However, autophagy induction also mediates mutant LRRK2 induced neurite shortening. Since PKA is neuroprotective against 6-hydroxydopamine, a PD neurotoxin, and suppresses autophagy in non-neuronal cells, I hypothesize that modulation of autophagy by PKA will protect against mutant LRRK2 induced injury. Furthermore, I hypothesize that PINK1, a mitochondrial kinase that regulates mitochondrial homeostasis and calcium buffering, will prevent neuronal injury caused by mutant LRRK2 by preventing mutant LRRK2-elicited mitochondrial dysfunction. The overall hypothesis is that injury elicited by mutant LRRK2 will be ameliorated by restoring mitochondrial homeostasis through autophagy modulation, improved mitochondrial function, and enhanced calcium buffering.

# 3.0 METHODS

## 3.1 TISSUE CULTURE

### 3.1.1 Mouse Cortical Neuron Isolation

Time-pregnant mice (Hilltop Laboratory Animals, Inc., Scottdale, PA, USA) were sacrificed when embryos were between E14-15 by cervical dislocation. The embryos were aseptically removed from the uterine horns and placed in ice-cold Dulbecco's phosphate buffered saline (DPBS) (Invitrogen, Carlsbad, CA, USA). The embryos were decapitated with a fresh, sterile scalpel, and the skull and meninges were dissected away from the brain. The cortex was isolated and digested with 100 units papain (Worthington Biochem. Corp. Lakewood, NJ, USA) in DPBS with 2-3 grains of L-cystein (Sigma-Aldrich Corp., St. Louis, MO, USA). The cells were triturated with fire-polished glass Pasteur Pipets (Fisher Scientific, Pittsburgh, PA, USA) and centrifuged at 200 x g. These steps were repeated two times to produce a single-cell suspension of cells. The digestion was terminated by adding 5mg/ml trypsin inhibitor (Worthington Biochem. Corp. Lakewood, NJ, USA), 10mM HEPES (BioWhittaker, Walkersville, MD, USA), 5mg/ml bovine serum albumin (Fisher Scientific, Pittsburgh, PA, USA) in Dulbecco's Modified Eagle Media (DMEM)/F-12 media (Invitrogen, Carlsbad, CA, USA). The cells were then plated on poly-lysine coated plates.

### 3.1.2 Mouse and Human Cell Culture

Mouse cortical neurons were cultured in Neurobasal (Invitrogen, Carlsbad, CA, USA), with 2mM Glutamax (Invitrogen, Carlsbad, CA, USA) and 2% B-27 supplement (Invitrogen, Carlsbad, CA, USA). Half of the media was refreshed every three days.

Human SH-SY5Y neuroblastoma, Human Embryonic Kidney 293 (HEK 293), and Human Cervical Carcinoma (HeLa) cell lines were cultured in DMEM (BioWhittaker, Walkersville, MD, USA) with 10% fetal calf serum (BioWhittaker, Walkersville, MD, USA), 2mM L-Glutamine (BioWhittaker, Walkersville, MD, USA), and 10mM HEPES (BioWhittaker, Walkersville, MD, USA). SH-SY5Y cells were differentiated with 10μM retinoic acid (Sigma-Aldrich Corp., St. Louis, MO, USA) for 3 days prior to transfection, and remained in media containing retinoic acid for the duration of the experiment. All cells were maintained at 37$^{o}$C with 5% $CO_2$, and the media was refreshed every three days.

All transfections were performed according to the manufacturer's protocol using Lipofectamine2000 (Invitrogen, Carlsbad, CA, USA). Briefly, Lipofectamine2000 and DNA plasmids or siRNA were added to separate tubes of OptiMEM (Invitrogen, Carlsbad, CA, USA) to incubate for 5 minutes. The OptiMEM/Lipofectamine mixture was then added to the DNA/siRNA. DNA/siRNA complexes with Lipofectamine were allowed to form for 15 minutes prior to adding the OptiMEM/Lipofectamine/DNA or siRNA mixture to the cells. The media was refreshed 24 hours after transfection.

### 3.1.3 Cell Culture Pharmacological Treatments

The following drugs were administered as indicated: 10μM Forskolin (Sigma-Aldrich Corp., St. Louis, MO, USA), 10 μM H89 (Merck KGaA, Darmstadt, Germany), 2μM rapamycin (LC Laboratories, Woburn, MA, USA), 250 μM cAMP (Sigma-Aldrich Corp., St. Louis, MO, USA), 0.5nM bafilomycin A (Merck KGaA, Darmstadt, Germany), 10nM FK506 (Enzo Life Sciences, Inc., Plymouth Meeting, PA, USA), 250nM okadaic acid (Merck KGaA, Darmstadt, Germany), 2mM EGTA (Sigma-Aldrich Corp., St. Louis, MO, USA), 2μM BAPTA-AM (Invitrogen, Carlsbad, CA, USA), 1μM NiCl (Sigma-Aldrich Corp., St. Louis, MO, USA), 1mM MPP+ (Sigma-Aldrich Corp., St. Louis, MO, USA), 50nM ω-agatoxin (Tocris Bioscience, Ellisville, MO, USA), 100nM ω-conotoxin (Tocris Bioscience, Ellisville, MO, USA), 10μM rolipram (Sigma-Aldrich Corp., St. Louis, MO, USA), and 1μM nitrendipine (Tocris Bioscience, Ellisville, MO, USA).

## 3.2 IMAGE ANALYSES

### 3.2.1 Immunocytochemistry

The cells were washed in phosphate buffered saline, pH 7.4 (PBS), and then incubated with 4% paraformaldehyde (Sigma-Aldrich Corp., St. Louis, MO, USA) in PBS for 15 minutes at room temperature. The cells were then washed twice with PBS and permeabilized in PBS with 0.1% Triton X-100 (Fisher Scientific, Pittsburgh, PA, USA) for one hour at room temperature. The

cells were incubated with SuperBlock (Thermo Scientific, Rockford, IL, USA) for one hour at room temperature to reduce non-specific antibody binding. Primary antibodies were added at the indicated dilutions (Table 1) for incubation overnight at 4$^{o}$C. The cells were washed three times in PBS, and then incubated with Alexafluor-488 or -546 conjugated secondary antibodies (1:1000) (Invitrogen, Carlsbad, CA, USA) for one hour at room temperature. The cells were then washed three times with PBS and imaged on an Olympus IX71 inverted microscope.

**Table 1: Antibodies and Dilutions for Immunocytochemistry**

| Antigen | Dilution | Company |
|---|---|---|
| GFP | 1:5000 | Invitrogen, Carlsbad, CA, USA |
| HA | 1:1000 | Covance, Emeryville, CA, USA |
| LC3 | 1:500 | Abgent Inc, San Diego, CA, USA |
| MAP2 | 1:1000 | Millipore, Billerica, MA, USA |
| PINK1 | 1:2000 | Invitrogen, Carlsbad, CA, USA |
| TOM20 | 1:200 | Santa Cruz Biotechnology, Santa Cruz, CA, USA |
| V5 | 1:1000 | Invitrogen, Carlsbad, CA, USA |

### 3.2.2 Neurite Length

For neurite length analysis, SH-SY5Y cells were fixed 48 hours after transfection and imaged by GFP fluorescence. For cortical neurons, cells were fixed 2 weeks after transfection and stained for GFP and MAP2 for dendrite length analysis. Neurite length was measured using NIH ImageJ.

### 3.2.3 Autophagosome Analysis

For image-based autophagy analysis, cells were fixed and imaged for either GFP-LC3 or LC3 immunofluorescence. The number of LC3-labeled autophagosomes was quantified per cell. LC3-labeled autophagosomes were identified as puncta 1.5 standard deviations above the mean cytoplasmic intensity.

### 3.2.4 Mitochondrial Content

Mitochondrial content was measured as the mitochondrial area, as indicated by either Cox8-GFP or Tom20 immunofluorescence, divided by the total cytoplasmic area of the compartment. In cortical neurons, mitochondrial content was measured in the soma, dendrites, and axons; for SH-SY5Y cells it was measured in the neurites and soma. NIH ImageJ was utilized to quantify the area of mitochondria and total area used for the mitochondrial content calculation.

### 3.2.5 Mitochondrial Trafficking

In the dendrites of cortical neurons, Cox8-GFP-labeled mitochondria were imaged every 20 seconds for a total of 2 minutes on days 2 and 4 after transfection. Images were captured on an inverted epifluorescence microscope (Olympus IX71) using Microsuite Five imaging software (Olympus). The neurons were imaged in PBS on a 37$^{o}$C warmed stage with a 40X dry objective. Using NIH ImageJ, the number of mitochondria moving anterograde, retrograde, or remained static was quantified as a percentage of the total mitochondria analyzed.

### 3.2.6 Mitochondrial Polarization

Cortical neurons were transfected at 7 DIV. Neurons were stained with 50nM tetramethylrhodamine methyl ester (TMRM) (Invitrogen, Carlsbad, CA, USA) and imaged in Krebs-Ringer buffer with 12.5nM TMRM on day 3 after transfection. Staining intensity was measured in the cytosol and mitochondria using ImageJ. Mitochondrial membrane potential ($\Psi$m) was calculated as the ratio of mitochondrial to cytosolic TMRM staining intensity as previously described.

### 3.2.7 Calcium Imaging

Cortical neurons were incubated with 5μM Fura2-AM (Invitrogen, Carlsbad, CA, USA) in normal buffer: 10mM HEPES pH 7.6, 140mM NaCl, 5mM KCl, 1mM $CaCl_2$, 1mM $MgCl_2$, and 10mM glucose at 37$^{o}$C for 1hr. Cells were washed in normal buffer for 10min, and then imaged

at 25°C. 50mM KCl in normal buffer was added to determine peak amplitude of calcium influx. To study calcium clearance, intracellular calcium was allowed to equilibrate in the presence of 50mM KCl in normal buffer; Fura2-AM intensity was then measured upon washout with normal buffer. The curve between the Fura2-AM staining at equilibrium with 50mM KCl and at baseline after KCl washout was fit by a mono-exponential equation, which was used to calculate the time constant (t).

## 3.3 BIOCHEMICAL ANALYSES

### 3.3.1 Immunoblotting

The cells were collected by scraping in scraping buffer: 25mM HEPES pH 7.5 (Research Organics, Inc., Cleveland, OH, USA), 50mM NaCl (Fisher Scientific, Pittsburgh, PA, USA), 5mM EDTA (Fisher Scientific, Pittsburgh, PA, USA), 2mM PMSF (Acros Organics, Geel, Belgium), and 1mM sodium orthovanadate (Sigma-Aldrich Corp., St. Louis, MO, USA). All cells were lysed in lysis buffer: 25mM HEPES pH 7.5, 150mM NaCl, 5mM EDTA, 10% glycerol (Acros Organics, Geel, Belgium), 1.0% Triton X-100, 2mM, 1mM sodium orthovanadate, 2mM sodium pyrophosphate, and 0.1mM E-64. After incubating cells in lysis buffer for 30 minutes on ice, lysates were centrifuged at 15,000 x g for 15 minutes. The supernatant was removed, and the Bradford Assay with Coomassie Plus (Thermo Scientific, Rockford, IL, USA) was used to quantify the protein concentration. 25μg of total protein was separated by SDS-PAGE and transferred to a PDVF membrane. After blocking the blots with 5% milk in PBS with 0.3% Tween 20 (PBST) (Fisher Scientific, Pittsburgh, PA, USA) for one hour

at room temperature, primary antibodies were added at the indicated dilutions (Table 2), and the blots were incubated overnight at 4°C. The blots were then washed with PBST three times and incubated with horseradish peroxidase-conjugate secondary antibodies (1:5000) (GE Healthcare, Piscataway, NJ, USA) for one hour at room temperature. The blots were washed three times with PBST and developed using SuperSignal West Pico (Thermo Scientific, Rockford, IL, USA) or ECL plus (GE Healthcare, Piscataway, NJ, USA).

**Table 2: Antibodies and Dilutions for Immunoblotting**

| Antigen | Dilution | Company |
|---|---|---|
| ADT2 | 1:500 | Santa Cruz Biotechnology, Santa Cruz, CA, USA |
| Atg3 | 2μg/ml | Sigma-Aldrich Corp., St. Louis, MO, USA |
| Atg7 | 1:1000 | Rockland Inc., Gilbersville, PA, USA |
| β-Actin | 1:5000 | Sigma-Aldrich Corp., St. Louis, MO, USA |
| GAPDH | 1:8000 | Abcam, Cambridge, MA, USA |
| GFP | 1:5000 | Invitrogen, Carlsbad, CA, USA |
| Lamin A/C | 1:1000 | Cell Signaling Technology, Danvers, MA, USA |
| LC3 | 1:500 | Nanotools, Teningen, Germany |
| LC3 C-terminus | 1:500 | Abgent Inc., San Diego, CA, USA |
| Phospho-LC3 S12 | 1:500 | Abgent Inc., San Diego, CA, USA |
| p62 | 1:100 | BD Biosciences, San Diego, CA, USA |
| VDAC | 1:500 | Merck KGaA, Darmstadt, Germany |

### 3.3.2 Immunoprecipitation

For hemagluttinin (HA)-tagged proteins, HEK 293 cells were lysed in PBS with 1.0% Triton X-100 and incubated with 1μg of anti-HA antibody (Covance, Emeryville, CA, USA) and protein A agarose beads (Invitrogen, Carlsbad, CA, USA) overnight at 4°C. The beads were collected by centrifugation at 500 x g for 5 minutes. The beads were washed and centrifuged 5 times, and

then the bound proteins were eluted with 2X SDS-PAGE sample buffer: 33mM Tris-HCl pH 6.8 (Fisher Scientific, Pittsburgh, PA, USA), 13.1% glycerol, 1% SDS (Bio-Rad, Hercules, CA, USA), 0.005% bromophenol blue (Fisher Scientific, Pittsburgh, PA, USA), and 25mM DTT (Sigma-Aldrich Corp., St. Louis, MO, USA).

For GFP-tagged proteins, HEK 293 or SH-SY5Y cells were lysed and processed according to the manufacturer's protocol for the μMACS Epitope Tag Protein Isolation Kit (Miltenyi Biotec, Auburn, CA, USA). Briefly, cells were lysed in μMACS lysis buffer on ice for 30 minutes. The samples were centrifuged at 10,000 x g for 10 minutes, and the supernatant transferred to a tube containing 50μl of anti-GFP MicroBeads. The samples were incubated for 30 minutes on ice prior to applying the samples to the μ Column on the μMACS Separator. The μ columns were washed with 900μl of μMACS lysis buffer. The bound proteins were eluted with hot μMACS elution buffer with 25mM DTT.

### 3.3.3 Two-Dimensional Gel Electrophoresis

The cells were lysed in lysis buffer as described above for immunoblotting. Proteins were acetone precipitated by adding 4 times the lysate volume of acetone (Sigma-Aldrich Corp., St. Louis, MO, USA) and incubating the mixture at -20$^{o}$C for 1-2 hours. The precipitate was collected by centrifugation at 15,000 x g for 15 minutes. The supernatant was removed and the pellet was allowed to dry at room temperature for 20 min. The pellet was then resuspended in rehydration buffer: 7M urea (Invitrogen, Carlsbad, CA, USA), 2M thiourea (Invitrogen, Carlsbad, CA, USA), CHAPS (Sigma-Aldrich Corp., St. Louis, MO, USA), and 25mM DTT. 50μg of protein with 4μl of pH 3-10 ampholytes (GE Healthcare, Piscataway, NJ, USA) in a

total volume of 125µl was then added to pH 3-10 IPG strips (GE Healthcare, Piscataway, NJ, USA).

The IPG strips underwent rehydration and isoelectric focusing (IEF) using a PROTEAN IEF cell (Bio-Rad, Hercules, CA, USA). After IEF, the IPG strips were reduced with Equilibration Buffer I (Bio-Rad, Hercules, CA, USA) and alkylated with Equilibration Buffer II (Bio-Rad, Hercules, CA, USA), and then loaded onto an SDS-PAGE gel as the second dimension. The proteins were transferred and blotted as described above.

### 3.3.4 Purification of Recombinant Proteins

To obtain purified LC3, recombinant GST-LC3 (gift of Drs. Masahiro Shibata and Yasuo Uchiyama, Osaka University) was induced using IPTG in DH5α bacteria and purified on an immobilized glutathione column (Thermo Scientific, Rockford, IL, USA) according to the manufacturer's specifications. To elute LC3 from the column, it was cleaved from the GST using Precision Protease (GE Healthcare, Piscataway, NJ, USA).

### 3.3.5 *In Vitro* Kinase Assay

For analysis of the PKA phosphorylation site on LC3, recombinant LC3 was incubated with recombinant PKA catalytic subunit (New England Biolabs Inc., Ipswich, MA, USA) for 2 hours at 30°C in 50mM Tris-HCl, 10mM $MgCl_2$ with 200µM ATP. To detect phosphorylation by autoradiography, the kinase reaction was supplemented with 300µCi/µmol ATP$\gamma^{32}$P.

### 3.3.6 Metabolic Labeling to Determine Phosphorylation in Cultured Cells

For detection of LC3 phosphorylation in cells, 293T cells were transfected with HA-LC3 followed by treatment with DMSO, 10μM forskolin, or 10μM forskolin and 10μM H89 in the presence of 1mCi/ml $^{32}P$ as $H_3{}^{32}PO_4$. All treatments were in the presence of 10μM rolipram, and for the final hour of incubation, 250nM okadaic acid and 10nM FK506. Cells were lysed in PBS with 1% Triton and proteins were immunoprecipitated and separated by SDS-PAGE as described above. Gels were silver stained and HA-LC3 bands were excised. $^{32}P$ incorporation was measured as counts/minute (Beckman LS3801) and normalized to band intensity.

### 3.3.7 Mass Spectrometry for Phosphosite and Protein Identification

For the identification of phosphorylation sites on LC3, gel bands were excised and destained in 100mM $NH_4(HCO_3)$. The proteins were reduced with 2.5mM tris(2-carboxyethyl)phosphine (Sigma-Aldrich Corp., St. Louis, MO, USA) for 15 minutes at 65$^{o}$C and alkylated with 3.75mM iodoacetamide (Sigma-Aldrich Corp., St. Louis, MO, USA) for 20 minutes at room temperature in the dark. Gel plugs were digested overnight with 8ng/μl chymotrypsin (Roche Diagnostics Corporation, Indianapolis, IN, USA) at room temperature. Peptides were extracted with 1:2 (vol/vol) 5% formic acid/acetonitrile. Samples were desalted using a $C_{18}$ ZipTip (Millipore, Billerica, MA, USA) and spotted for mass spectrometric analysis on a 4800 MALDI-TOF/TOF Analyzer (AB SCIEX, Foster City, CA, USA). Peptide phosphorylation was detected as a gain of 80Da by MALDI-TOF-MS. Amino acid sequences were identified by subjecting peptides to

collision-induced dissociation during MS/MS. The loss of phosphoric acid (98Da) was indicative of phosphorylation during MS/MS.

For the identification of LC3 or PINK1 interacting proteins, GFP-tagged LC3 or PINK1 were immunoprecipitated as described above. Proteins were separated by SDS-PAGE and excised bands were processed for mass spectrometry. Proteins were identified in the SwissProt 57.13 database limited to Metazoan organisms using the Mascot algorithm on Matrix Science (Mascot Server 2.3) with the search parameters listed in table 3. The requirements for protein identification included: presence of 2 or more unique peptides and a Mascot score greater than 62 ($p<0.05$).

**Table 3: Mascot Search Parameters for Protein Identification**

| | |
|---|---|
| Type of Search | : MS/MS Ion Search |
| Enzyme | : Chymotrypsin |
| Fixed Modification | : Carbamidomethyl (C) |
| Variable Modification | : Oxidation (M) |
| Mass Values | : Monoisotopic |
| Protein Mass | : Unrestricted |
| Peptide Mass Tolerance | : ±50ppm |
| Fragment Mass Tolerance | : ±0.5Da |
| Max Missed Cleavages | : 2 |
| Instrument Type | : MALDI-TOF-TOF |

### 3.3.8 Microtubule Isolation

Cortical neurons were washed with PBS, then lysed in cytoskeleton stabilization buffer: 10mM PIPES pH 6.8, 50mM KCl, 2mM EGTA, 1mM $MgCl_2$, 2M glycerol, and 0.5% Triton X-100 for 15 minutes at room temperature. The lysate was removed and centrifuged at 16,000 x g to collect polymerized tubulin in the pellet. The supernatant containing free tubulin was removed and labeled as the cytoplasmic fraction. Cytoskeleton stabilization buffer containing 0.5% SDS was added to the plate of neurons to collect polymerized tubulin. This was then added to the previous pellet containing polymerized tubulin and was labeled as microtubule fraction. The fractions were then immunoblotted as described above.

## 3.4 STATISTICAL ANALYSIS

The student's *t* test was used to compare means between two groups. For comparisons between more than two groups, data was analyzed by one-way ANOVA with a Bonferroni correction for multiple comparisons. A p-value less than 0.05 was considered significant.

# 4.0 RESULTS

## 4.1 LRRK2 NEURONAL DEGENERATION: A CELL CULTURE MODEL

### 4.1.1 Mutant LRRK2 causes a depletion of dendritic mitochondria

Since mitochondrial dysfunction has been implicated in PD, mitochondrial homeostasis was assessed by measuring the mitochondrial content levels in the soma, dendrites, and axons of cortical neurons using a mitochondrial marker, Cox8-GFP (Fig. 1A). Mutant LRRK2, but not wild type, significantly reduced the mitochondrial content in dendrites at 5 days after transfection (Fig. 1B), but not in the axons (Fig. 1E). This reduction in mitochondrial content was not due to a reduction in dendrites, since the dendritic area was similar in all groups (Fig. 1C). Interestingly, only the G2019S mutation affected the somatic mitochondrial content (Fig. 1D). Mutant LRRK2 expression also caused a reduction in neuritic mitochondrial content in SH-SY5Y cells using endogenous TOM20 staining (Fig. 3D).

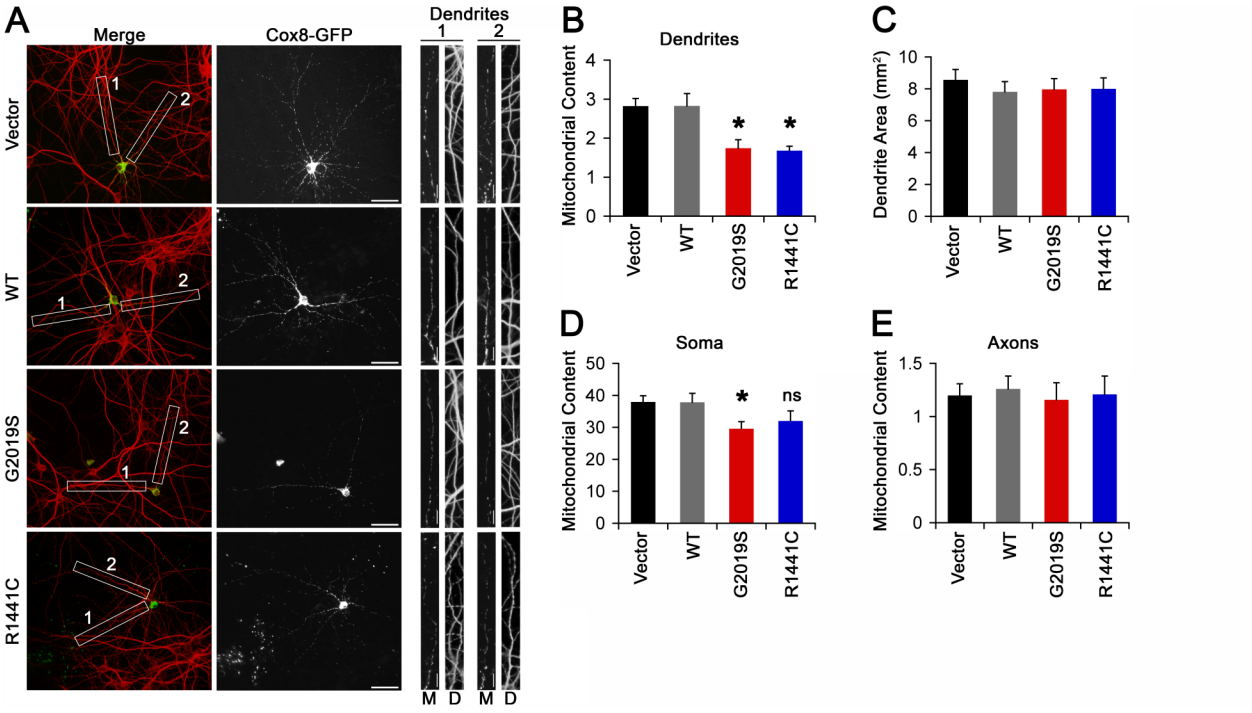


**Figure 1: Mutant LRRK2 depletes dendritic mitochondria.**
(A) Representative images of cortical neurons expressing vector or LRRK2 with Cox8-GFP. Dendrites were identified by MAP2 staining. Scale bar=50μm. Inset: 2X zoom of proximal dendrites showing a decrease in mitochondrial content in mutant LRRK2 groups. M=Mitochondria (green channel) and D=Dendrite (red channel). Scale bar=50μm. (B) Quantification of mitochondrial content (mitochondrial pixels/dendrite pixels) in dendrites (mean±SEM; n=19-32 neurons/group compiled from 3 independent experiments). *p<0.05 vs. vector (C) Quantification of dendrite area (mean±SEM; n=19-32 neurons/group compiled from 3 independent experiments). (D-E) Quantification of mitochondrial content in the soma and axons (mean±SEM; n=14-32 neurons/group compiled from 3 independent experiments). *p<0.05 vs. vector; ns=not significant vs. vector.

### 4.1.2 Mutant LRRK2 does not cause defects in mitochondrial trafficking

Dendritic mitochondrial content is controlled by biogenesis, degradation, and trafficking[84]. To determine if mutant LRRK2 disrupted mitochondrial trafficking, mitochondrial movement was measured in dendrites of cortical neurons. Mitochondrial that had a net movement away from the soma were classified as anterograde, and those that moved toward the soma were retrograde. If a mitochondrion did not move during the 2-minute imaging period, it was labeled as stationary.

There were no differences in mitochondrial trafficking between LRRK2 mutants and vector control (Fig. 2A-C).

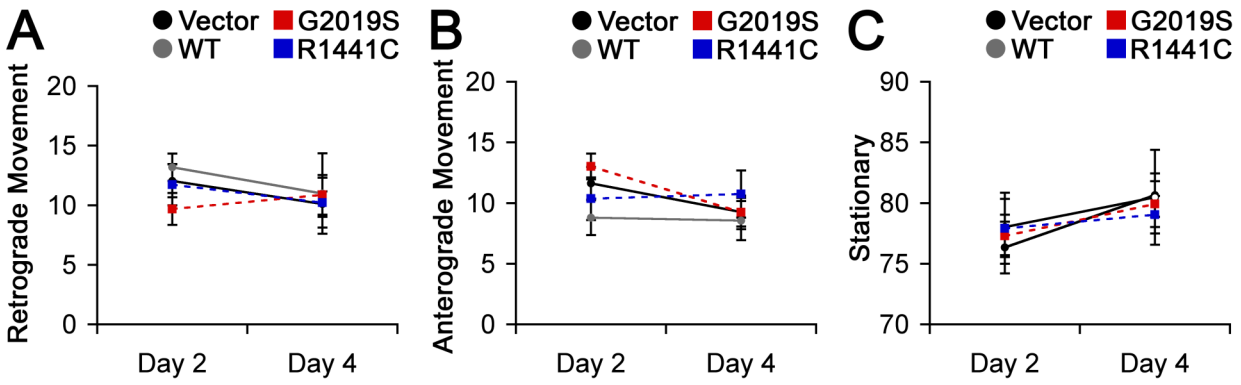


**Figure 2: Mutant LRRK2 does not perturb mitochondrial traffic.**
(A-C) Mitochondrial movement was tracked using Cox8-GFP in the proximal dendrites of cortical neurons over a 2 minute time period (mean±SEM; n=6-17 neurons/group compiled from 3 independent experiments). Mitochondrial movement was quantified as retrograde (movement towards the soma), anterograde (movement away from the soma), or stationary (no net movement).

### 4.1.3 Mutant LRRK2 induces depolarization and autophagic degradation of mitochondria

The effects of mutant LRRK2 on mitochondrial degradation, which is primarily executed by the autophagy pathway, was investigated next. Using the autophagosome marker, GFP-LC3, mutant LRRK2 elicited an increase in autophagosomes in neurons (Fig. 3A). Inhibition of autophagic degradation with bafilomycin A (Baf A) for 48 hours prevented the decreased in mitochondrial content caused by mutant LRRK2 (Fig. 3B). The effects of Baf A on autophagy were verified by immunoblotting for LC3. A decrease in autophagic degradation leads to an increase in autophagosomes and the LC3-II bound to autophagosomes (Fig. 3C). Autophagy induction was also inhibited autophagy induction using RNAi against the essential autophagy protein, Atg7. Similar to Baf A, RNAi against Atg7 prevented the reduction in mitochondrial content induced

by mutant LRRK2 (Fig. 3D). The efficiency of Atg7 knockdown and verification of autophagy inhibition was measured by immunoblotting (Fig. 3E). Decreased LC3-II levels are indicative of a reduction in autophagy induction.

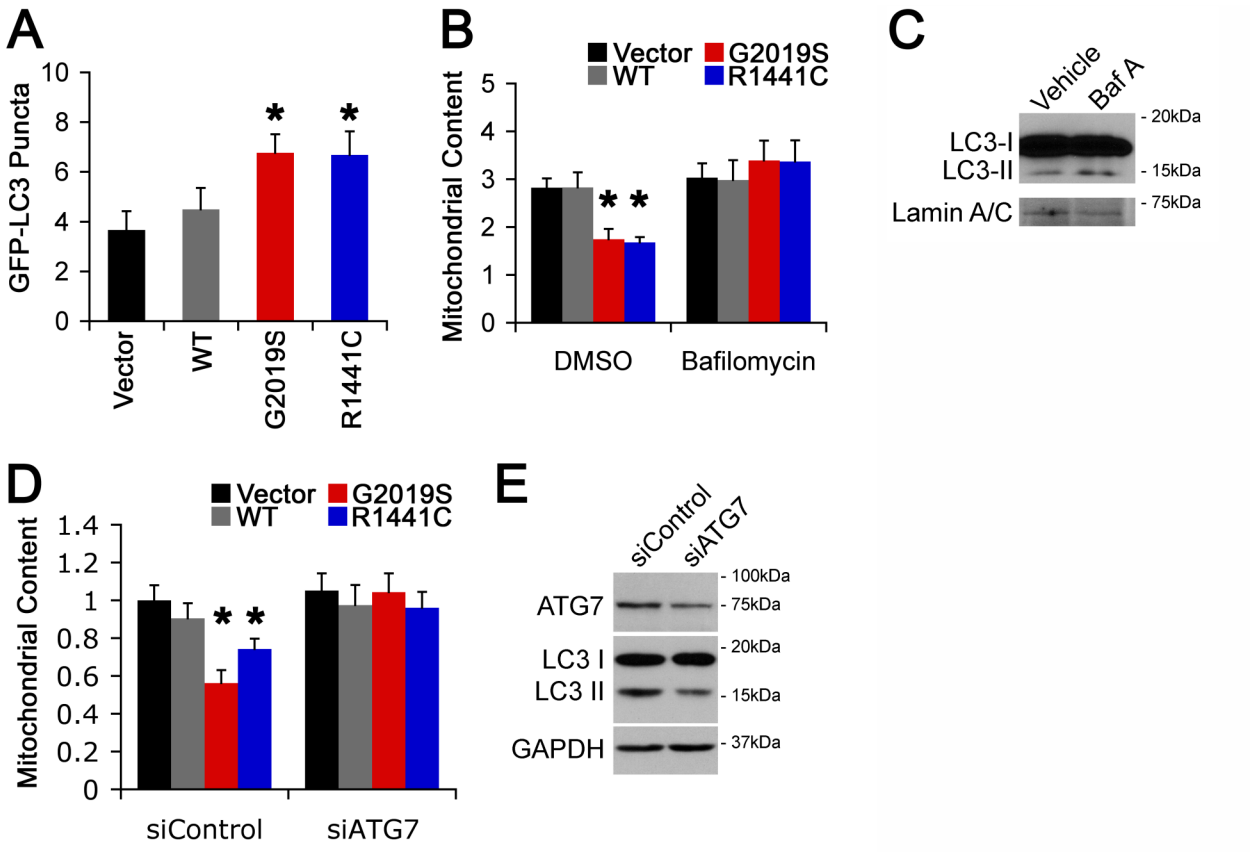


**Figure 3: Mutant LRRK2 induces mitochondria degradation via autophagy.**
(A) Steady state autophagy levels were measured by counting the number of GFP-LC3 labeled autophagosomes (mean±SEM; n=20-30 neurons/group compiled from 3 independent experiments). *p<0.05 vs. vector. (B) Mitochondrial content was quantified in proximal dendrites in the presence and absence of bafilomycin A, an inhibitor of lysosomal fusion (mean±SEM; n=5-32 neurons/group compiled from 3 independent experiments). *p<0.05 vs. vector. (C) Verification that bafilomycin A (Baf A) inhibits autophagic degradation. Inhibition of degradation is indicated by the increase in LC3-II. (D) Mitochondrial content was measured in the neurites of SH-SY5Y cells in the presence or absence of RNAi against Atg7 (mean±SEM; n=26-58 cells/group compiled from 3 independent experiments).. *p<0.05 vs. vector. (E) Verification of RNAi-mediated reduction in Atg7; reduction in LC3-II indicates that RNAi against Atg7 inhibits autophagy induction.

Mitochondrial depolarization has been identified as a signal to induce mitophagy[85]. To determine if mutant LRRK2 affected mitochondrial polarization, TMRM staining intensity was measured in the dendrites of neurons expressing mutant LRRK2. TMRM is a mitochondrial membrane potential-dependent dye, and mitochondrial polarization is directly proportional to the intensity of TMRM staining[14]. Mutant LRRK2, but not wild type, caused mitochondrial depolarization 3 days after transfection (Fig. 4A-B). The reduction in membrane potential precedes mitochondrial degradation since there is no difference in the area of proximal dendrite occupied by Cox8-GFP-labeled mitochondria at 3 days after transfection (Fig. 4C).

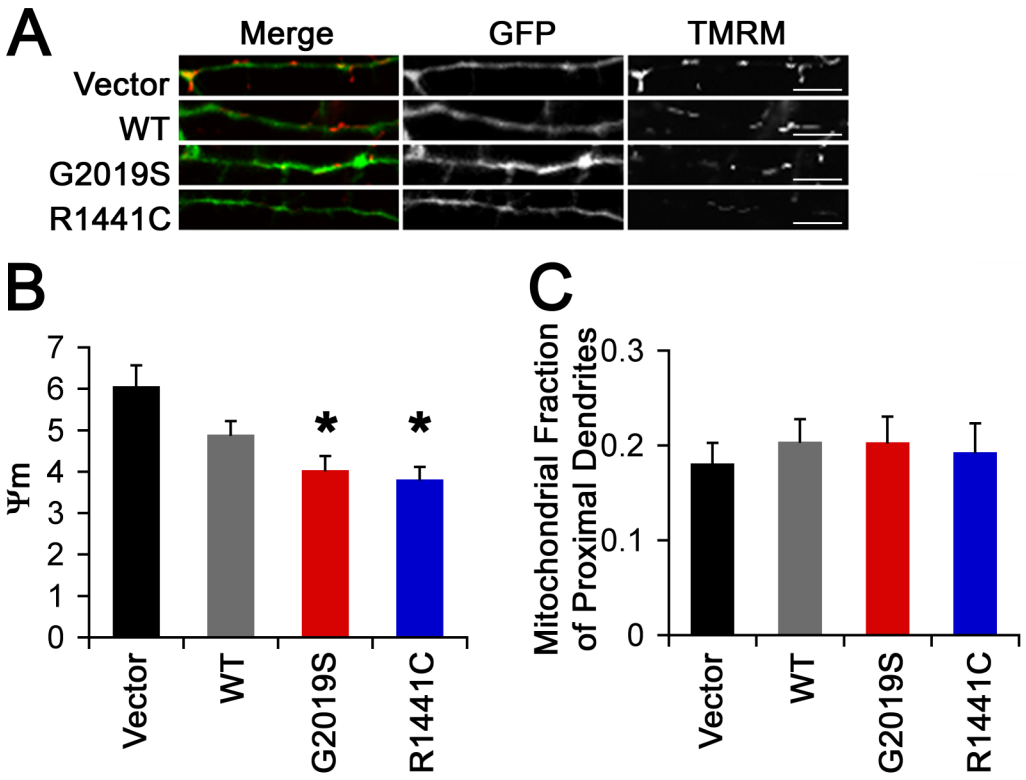


**Figure 4: Mutant LRRK2 elicits mitochondrial depolarization.**
(A) Representative images of proximal dendrites stained with TMRM. Scale bar=20μm. (B) Quantification of mitochondrial membrane potential (Ym) as mitochondrial TMRM intensity divided by cytosolic TMRM intensity (mean±SEM; n=16-29 neurons/group compiled from 3 independent experiments).. *p<0.05 vs. vector. (C) Quantification of area occupied by mitochondria divided by dendrite area (mean±SEM; n=16-29 neurons/group compiled from 3 independent experiments).

### 4.1.4 Depletion of mitochondria precedes dendrite retraction

As a measure of neuronal degeneration, total dendrite length was measured in neurons expressing mutant LRRK2. Mutant LRRK2, but not wild type, induced a reduction in dendrite length between 7-14 days after transfection (Fig. 5A-B). The dendrite degeneration is therefore downstream of mitochondrial depolarization and mitophagy elicited by mutant LRRK2. Moreover, inhibition of autophagy in SH-SY5Y cells, which prevents mitochondrial degradation, attenuated the neurite shortening elicited by mutant LRRK2 and MPP+, a neurotoxin model of PD (Fig. 5C).

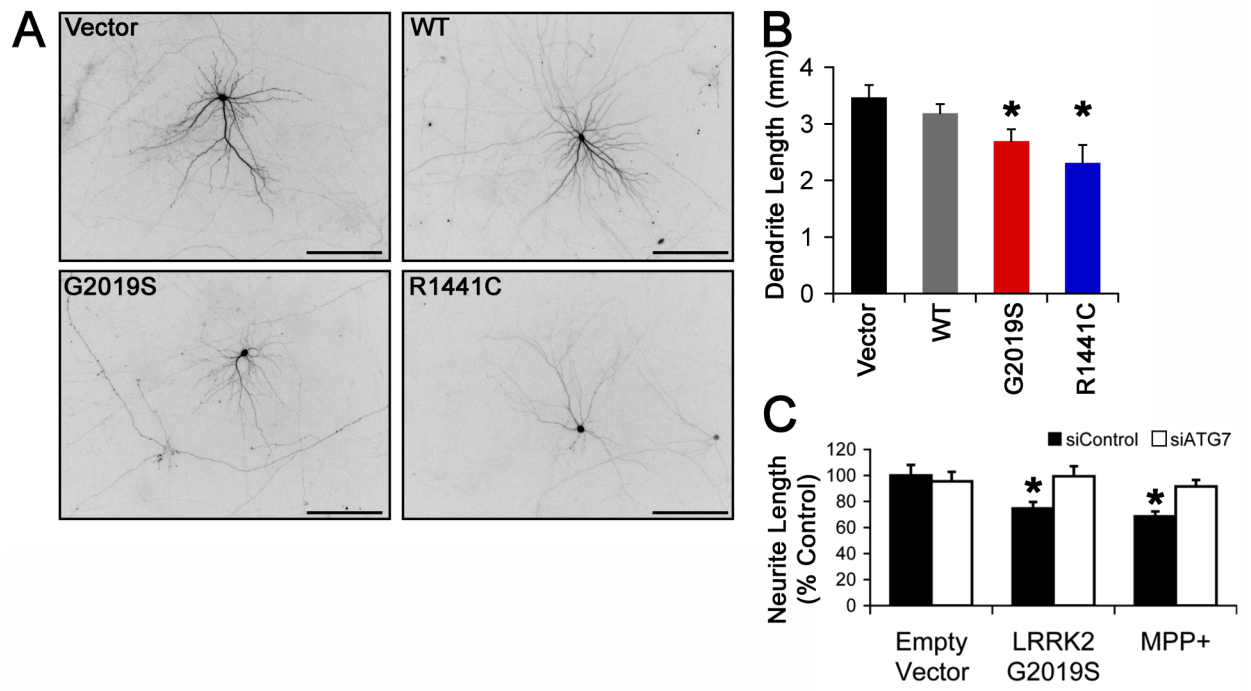


**Figure 5: Mutant LRRK2 induces autophagy-mediated neurite shortening.**
(A) Representative images of neurons expressing GFP and vector or LRRK2. Scale bar=100μm. (B) Quantification of dendrite length in cortical neurons (mean±SEM; n=10-35 neurons/group compiled from 3 independent experiments). *p<0.05 vs. vector. (C) Quantification of neurite length in SH-SY5Y cells expressing mutant LRRK2 or treated with MPP+ for 24hrs (mean±SEM; n=50-100 cells/group compiled from 3 independent experiments). *p<0.05 vs. Empty vector siControl.

## 4.2 PINK1 PROTECTS AGAINST LRRK2-MEDIATED DEGENERATION

### 4.2.1 PINK1 prevents autophagy, mitochondrial degradation, and neurite retraction caused by mutant LRRK2

Since mutant LRRK2 disrupts mitochondrial homeostasis, the effects of PINK1, which maintains mitochondrial homeostasis and provides protection against toxin insults, on mutant LRRK2 were assessed. Overexpression of wild type PINK1, but not the PD-associated L489P mutant, prevented neurite shortening in SH-SY5Y cells caused by LRRK2 G2019S (Fig. 6A). Stable expression of wild type PINK1 in SH-SY5Y cells also prevented the autophagy induction and neuritic mitophagy elicited by LRRK2 G2019S (Fig. 6B). Furthermore, stable expression of wild type PINK1 prevented the autophagy induction and neuritic mitochondrial degradation (Fig. 6C-D). Similar to cortical neurons, the mitochondrial degradation occurred primarily in the neurites, as there was no decrease in somatic mitochondrial content (Fig. 6E).

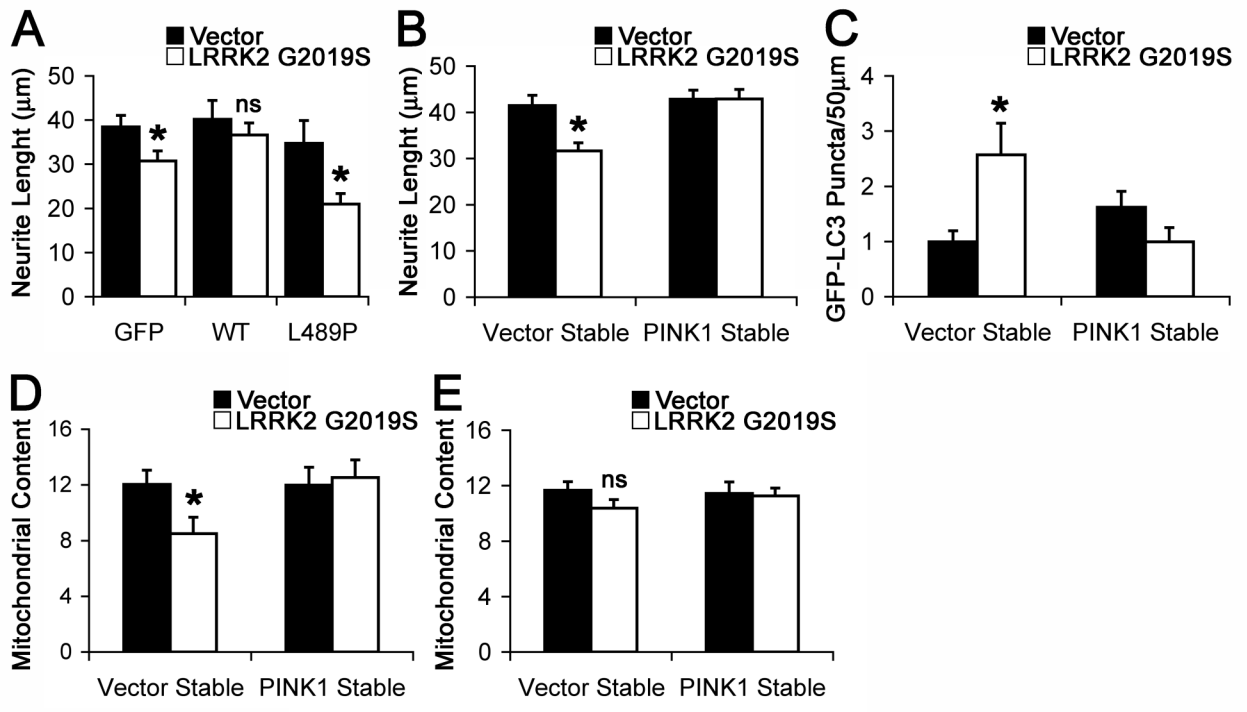


**Figure 6: PINK1 prevents neurite retraction, autophagy induction and mitochondrial degradation elicited by mutant LRRK2.**
(A) Quantification of neurite lengths in SH-SY5Y cells expressing vector or LRRK2 G2019S and GFP or WT or L489P PINK1-GFP (mean±SEM; n=12-57 cells/group compiled from 2 independent experiments). *p<0.05 vs. corresponding vector group; ns=not significant. (B) Quantification of neurite lengths in SH-SY5Y cells stably expressing vector or PINK1 (mean±SEM; n=145-158 cells/group compiled from 3 independent experiments). *p<0.05 vs. vector transfected vector cell line. (C) Quantification of GFP-LC3 labeled autophagosomes in cells stably expressing vector or PINK1 (mean±SEM; n=92-116 cells/group compiled from 3 independent experiments). *p<0.05 vs. vector transfected vector cell line. (D-E) Quantification of neuritic or somatic mitochondrial content in cells stably expressing vector or PINK1 (mean±SEM; n=43-53 cells/group compiled from 3 independent experiments). *p<0.05 vs. vector transfected vector stable cell line; ns=not significant.

### 4.2.2 PINK1 levels regulate the phosphorylation of Drp1 and LC3

To determine the signaling mechanism(s) underlying PINK1-mediated neuroprotection, a 2-D gel electrophoresis approach was utilized to attempt to identify PINK1 substrates. The lysates from SH-SY5Y cells stably expressing an shRNA hairpin against PINK1 or a scrambled sequence were separated 2-D SDS-PAGE. The results indicated that a protein that regulates mitochondrial homeostasis, Drp1, and an essential autophagy protein, LC3, showed a spot pattern indicative of dephosphorylation in cells expressing PINK1 shRNA (Fig. 7A-B). *In vitro*

kinase assays were preformed to assess whether PINK1 directly phosphorylated either of these proteins; however, neither protein was a direct substrate for PINK1.

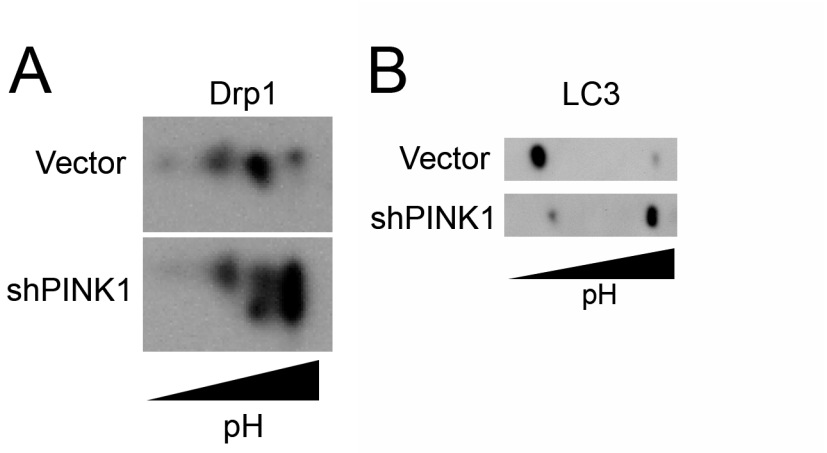


**Figure 7: PINK1 expression level alters the phosphorylation status of Drp1 and LC3.**
(A-B) 2-D immunoblots from SH-SY5Y cells stably expressing scrambled shRNA or PINK1 shRNA. Blots were probed for Drp1 or LC3. Increased phosphorylation status is correlated with increased staining intensity at lower pHs. Immunoblots represent 1 experiment.

## 4.3 PKA PHOSPHORYLATES LC3 AND PREVENTS PARKINSONIAN NEURONAL DEGENERATION

### 4.3.1 PKA suppresses autophagy induction and provides neuroprotection

Since the phosphoregulation of Drp1 has been established, the phosphoregulation of LC3 was further investigated. Bioinformatic analysis identified consensus phosphorylation sites on LC3 (Table 4). Since PKA provides protection against the neurotoxin, 6-hydroxydopamine, and suppresses autophagy induction in yeast and hepatocytes[75, 81, 82], the effects of PKA on LC3

phosphorylation and autophagy regulation were measured. Therefore, the effects of PKA on autophagy were first assessed in neuronal cells.

**Table 4: Phosphorylation Site Prediction for LC3**

| Site | Kinase | Score |
|---|---|---|
| S3 | Protein kinase C | 0.66 |
| T6 | Protein kinase C | 0.86 |
| S12 | Protein kinase C | 0.50 |
| S12 | Protein kinase A | 0.61 |
| T93 | p38MAPK | 0.53 |
| T93 | cdk5 | 0.53 |
| S96 | Casein kinase II | 0.54 |
| Y99 | Insulin Receptor | 0.51 |
| S101 | Casein kinase II | 0.62 |
| Y110 | Insulin Receptor | 0.52 |
| S115 | DNA Protein kinase | 0.62 |
| S115 | ATM | 0.57 |
| T118 | Casein kinase I | 0.52 |

To determine if PKA activation regulates autophagy in neuronal cells, SH-SY5Y cells expressing GFP-RFP-LC3 were treated with rapamycin in the presence or absence of cAMP. The GFP-RFP-LC3 construct allows for analysis of autophagic flux, i.e., distinguishing between the inhibition of autophagy induction and the increase in autophagosome maturation, as both processes could lead to a decrease in the number of GFP-LC3 labeled autophagosomes. Early autophagosomes are GFP-RFP dual fluorescent puncta, which appear yellow, but late autophagosome are RFP only, since the acidic environment of the lysosome quenches the GFP fluorescence. Treatment with cAMP reduced the number of early autophagosomes after 1 hour of treatment with rapamycin; however, neither rapamycin nor cAMP had an effect on late autophagosomes at this time (Fig. 8A-B). cAMP also reduced the numbers of early and late

autophagosomes after 3 hours of rapamycin (Fig. 8C). These results indicate that cAMP activation of PKA suppresses autophagy induction rather than enhancing autophagosome maturation.

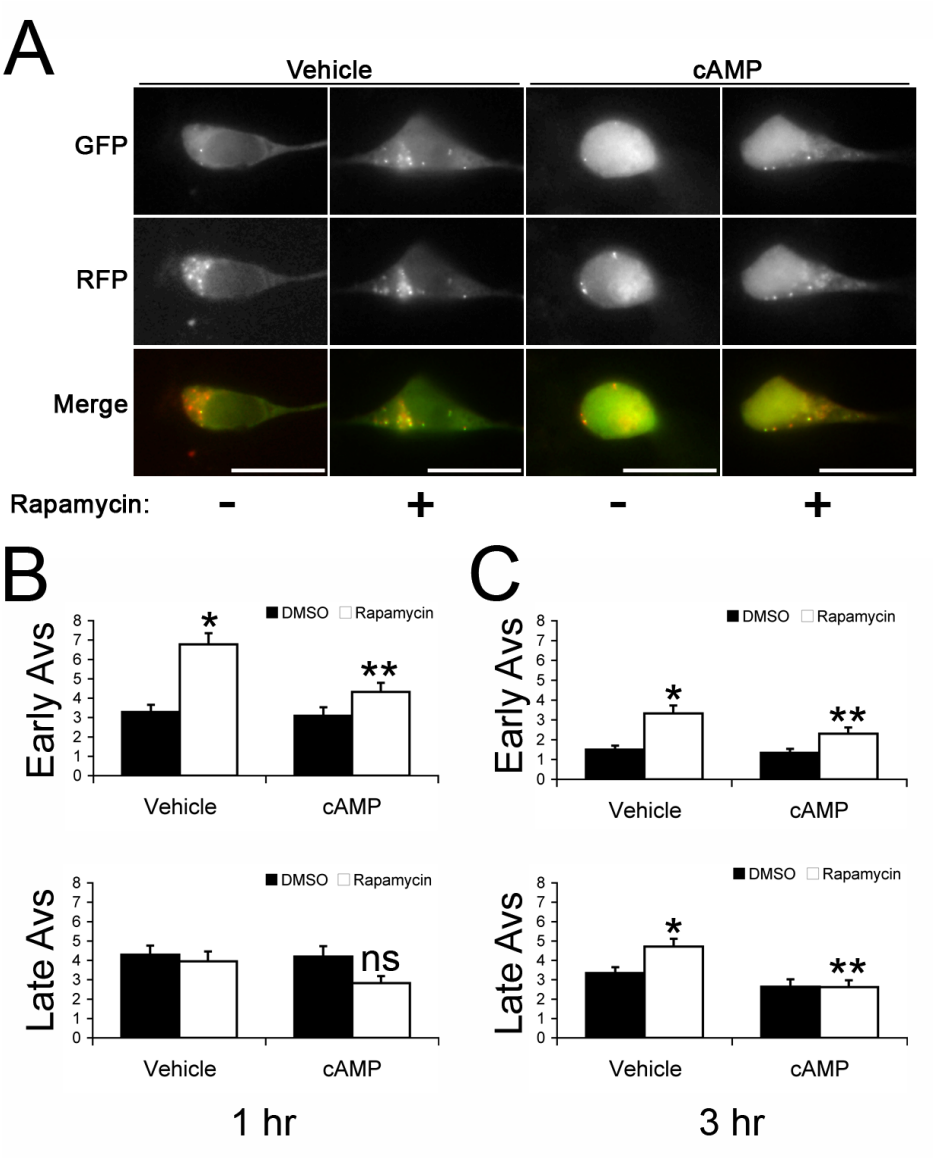


**Figure 8: cAMP suppresses autophagy induction.**
(A) Representative images of SH-SY5Y cells expressing RFP-GFP-LC3 treated with rapamycin and/or cAMP for 1hr. Scale bar=20μm. (B-C) Quantification of early (yellow puncta) and late (red puncta) autophagosomes after 1 or 3 hr of rapamycin and/or cAMP treatment (mean±SEM; n=50-55 cells/group compiled from 3 independent experiments). *p<0.05 vs. DMSO vehicle group, **p<0.05 vs. rapamycin vehicle group, and ns=not significant.

Treatment with cAMP also suppressed autophagy induced by MPP+ and the LRRK2-G2019S mutation, two models of PD (9A-C). Furthermore, cAMP prevented neurite shortening in both models (Fig. 9D-E), indicating that autophagy inhibition by PKA activation provides neuroprotection. Utilizing subcellularly targeted of PKA the effects of nuclear and cytoplasmic PKA on autophagy suppression and neuroprotection were assessed. Untargeted PKA and cytoplasmic-targeted PKA (PKA-NES) equally suppressed autophagy induction elicited by rapamycin or LRRK2-G2019S, but nuclear-targeted PKA (PKA-NLS) failed to suppress autophagy induction (Fig. 10A-B). Similarly, only the untargeted PKA and cytoplasmic-targeted PKA prevented neurite shortening (Fig. 10C). These results suggest that PKA phosphorylates a cytoplasmic protein to suppress autophagy, which supports the hypothesis that PKA may phosphorylate LC3 to prevent mutant LRRK2 induced neuronal injury.

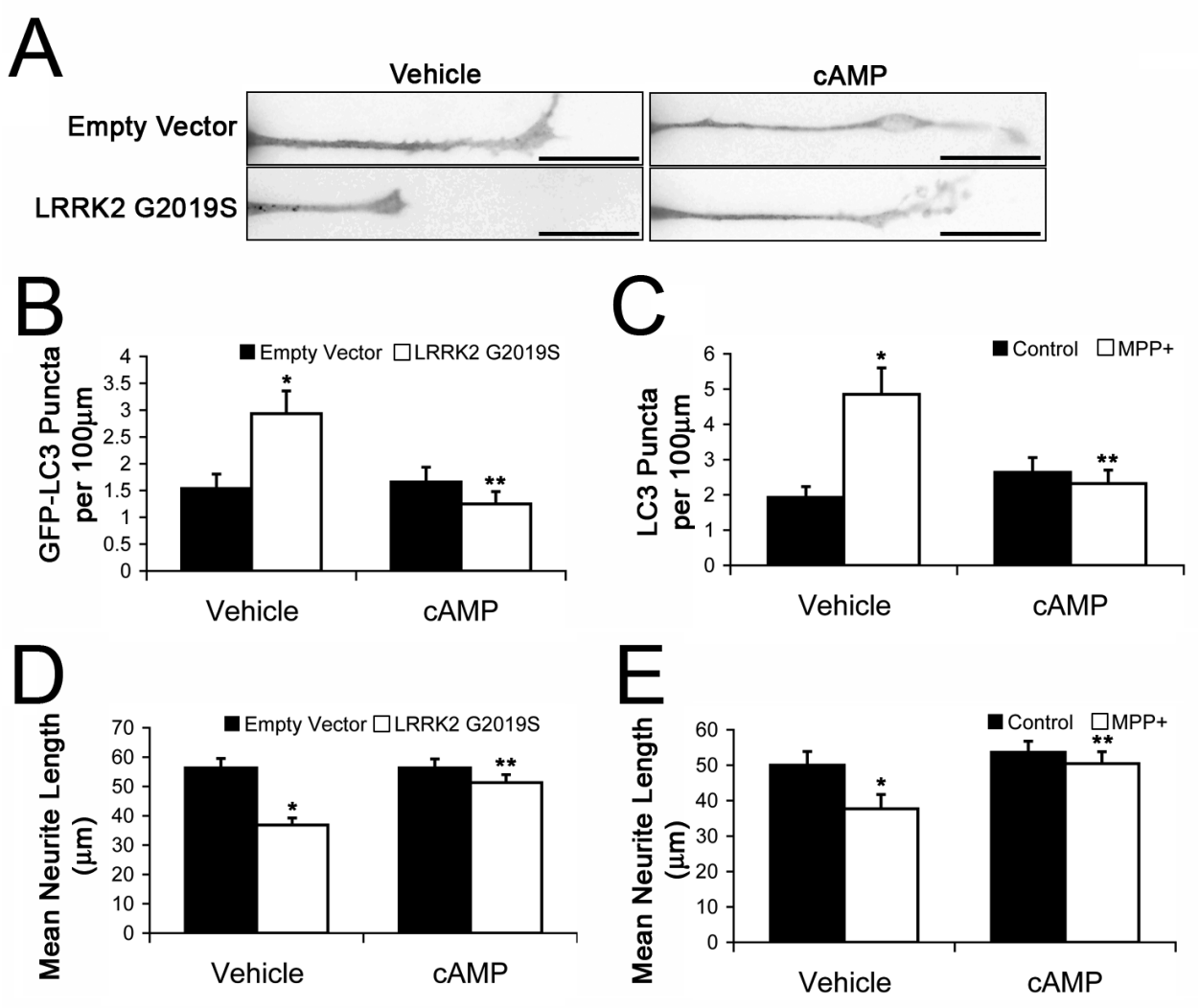


**Figure 9: cAMP suppresses autophagy and prevents neurite shortening.**
(A) Representative images of neurites from SH-SY5Y cells expressing GFP-LC3 and vector or LRRK2 G2019S in the presence or absence of cAMP. Bright GFP-LC3 puncta (>1.5 standard deviations above mean cytoplasmic fluorescence) were considered autophagosomes. Scale bar=20µm. (B-C) Quantification of GFP-LC3 labeled autophagosomes in SH-SY5Y cells expressing vector or LRRK2 G2019S (mean±SEM; n=80-90 cells/group compiled from 3 independent experiments) or treated with or without MPP+ (mean±SEM; n=50-55 cells/condition compiled from 3 independent experiments) in the presence and absence of cAMP. *p<0.05 vs. vehicle vector or control; **p<0.05 vs. vehicle LRRK2 G2019S or MPP+. (D-E) Quantification of neurite lengths in SH-SY5Y cells expressing vector or LRRK2 G2019S (mean±SEM; n=80-90 cells/condition compiled from 3 independent experiments) or treated with or without MPP+ (mean±SEM; n=50-60 cells/condition compiled from 3 independent experiments) in the presence or absence of cAMP. *p<0.05 vs. vehicle vector or control; **p<0.05 vs. vehicle LRRK2 G2019S or MPP+.

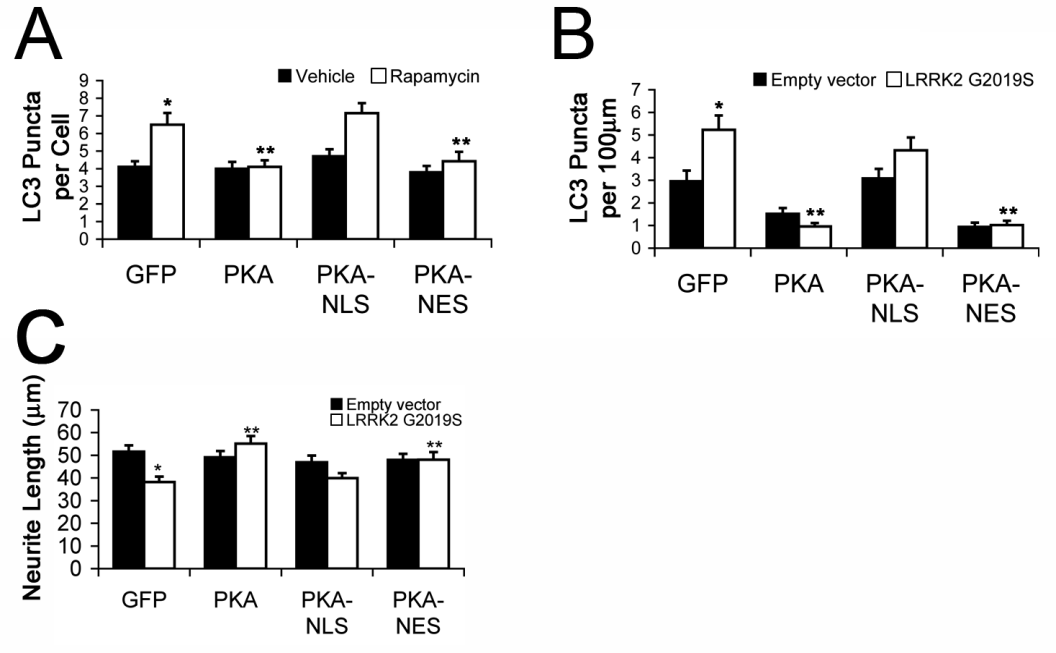


**Figure 10: Cytoplasmic PKA suppresses autophagy and prevents neuronal injury.**
(A) Quantification of endogenous LC3-labeld autophagosomes in SH-SY5Y cells in the presence and absence of rapamycin (mean±SEM; n=35-45 cells/group compiled from 3 independent experiments). *p<0.05 vs. GFP vehicle group; **p<0.05 vs. GFP rapamycin group. (B) Quantification of endogenous LC3-labeled autophagosomes in SH-SY5Y cells expressing vector or LRRK2 G2019S (mean±SEM; n=80-90 cells/group compiled from 3 independent experiments). *p<0.05 vs. GFP vector group; **p<0.05 vs. GFP LRRK2 G2019S group. (C) Quantification of neurite lengths in SH-SY5Y cells expressing vector or LRRK2 G2019S (mean±SEM; n=90-130 cells/group compiled from 3 independent experiments). *p<0.05 vs. GFP vector group; **p<0.05 vs. GFP LRRK2 G2019S group. PKA-NLS=nuclear-targeted PKA; PKA-NES=cytoplasmic-targeted PKA.

### 4.3.2 Identification of the PKA phosphorylation site on LC3

To determine if PKA phosphorylates LC3, 2-D immunoblotting as performed on neurons in the presence or absence of forskolin, an activator of adenylyl cyclase, which produces cAMP and stimulates PKA. Forskolin treatment increased the staining intensity of the more acidic spot, indicative of increased phosphorylation (Fig. 11A). HEK293 cells expressing HA-LC3 were then rabiolabeled in the presence of forskolin or forskolin and the PKA inhibitor, H89. HA-LC3 was then immunoprecipitated and the incorporation of $^{32}P$ was measured. Forskolin increased the incorporation of $^{32}P$ into LC3, which was reduced by H89 (Fig. 11B), indicating that PKA

increases the phosphorylation of LC3 in cultured cells. Finally an *in vitro* kinase assay was used to determine if PKA directly phosphorylated LC3. Recombinant PKA and LC3 were incubated together with ATP-$\gamma^{32}$P and then separated by SDS-PAGE. Indeed, incubation with PKA increased the phosphorylation of LC3 as detected by autoradiogram (Fig. 11C), verifying that LC3 is a direct substrate of PKA.

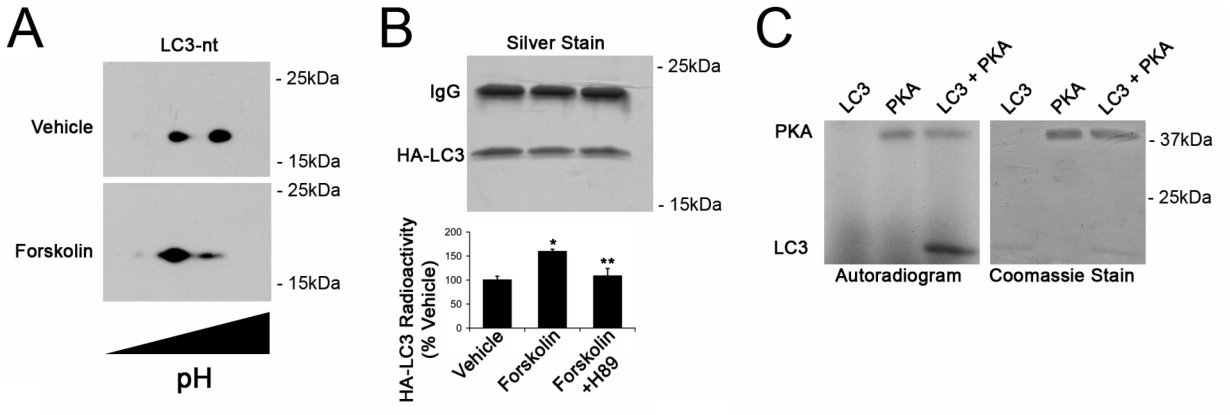


**Figure 11: PKA phosphorylates LC3.**
(A) 2-D immunoblot from cortical neurons treated with or without forskolin for 1hr. Blots were probed for LC3, and increased phosphorylation status is indicated by an increased staining intensity of the more acidic spots. Immunoblots represent 1 experiment. (B) Immunoprecipitation of HA-LC3 from cells treated with vehicle, forskolin, or forskolin and H89 for 5hrs in the presence of $^{32}$P-inorganic phosphate. Bands were excised from the gel, and radioactivity incorporation was quantified using a scintillation counter. Image is representative of 3 independent experiments; graphical data is mean±SEM with 1 lane/group compiled from 3 independent experiments. *$p<0.05$ vs. vehicle; **$p<0.05$ vs. forskolin. (C) *In vitro* kinase assay with recombinant PKA and LC3 in the presence of ATPg$^{32}$P. Radioactivity was measured by autoradiography. Autoradiogram is representative of 2 independent experiments.

To determine the function of LC3 phosphorylation, the PKA phosphorylation site was identified by mass spectrometry. Cold *in vitro* kinase assays were subjected to MALDI-TOF-MS, and phosphopeptides were identified by the indicative 80Da shift due to the addition of phosphate. Incubation with PKA produced a peak at m/z 901.41 that was not present in LC3 alone (Fig. 12A-B). This appearance of the peak at m/z 901.41 was accompanied by the loss of

the peak at m/z 821.33 (Fig. 12A-B). Analysis by MS/MS identified the peaks at m/z 821.33 and 901.41 as the amino acid sequence KQRRSF spanning the LC3 residues 8-13. The shift of 80Da is indicative of a phosphorylation; this was confirmed by MS/MS analysis, which showed the loss of the phosphate from S12 when the m/z 901.41 peak was subjected to collision-induced dissociation (Fig. 12C). Together these data suggest that PKA phosphorylates LC3 at the S12 residue. To verify that this is the only PKA site, an *in vitro* kinase assay was performed with an S12A mutant. Deletion of this phosphorylation site abolished PKA phosphorylation of LC3 (Fig. 12D). Furthermore, using an antibody developed against the PKA phosphorylation site on LC3, the forskolin-induced phosphorylation of endogenous LC3 was detected in neurons (Fig. 12E).

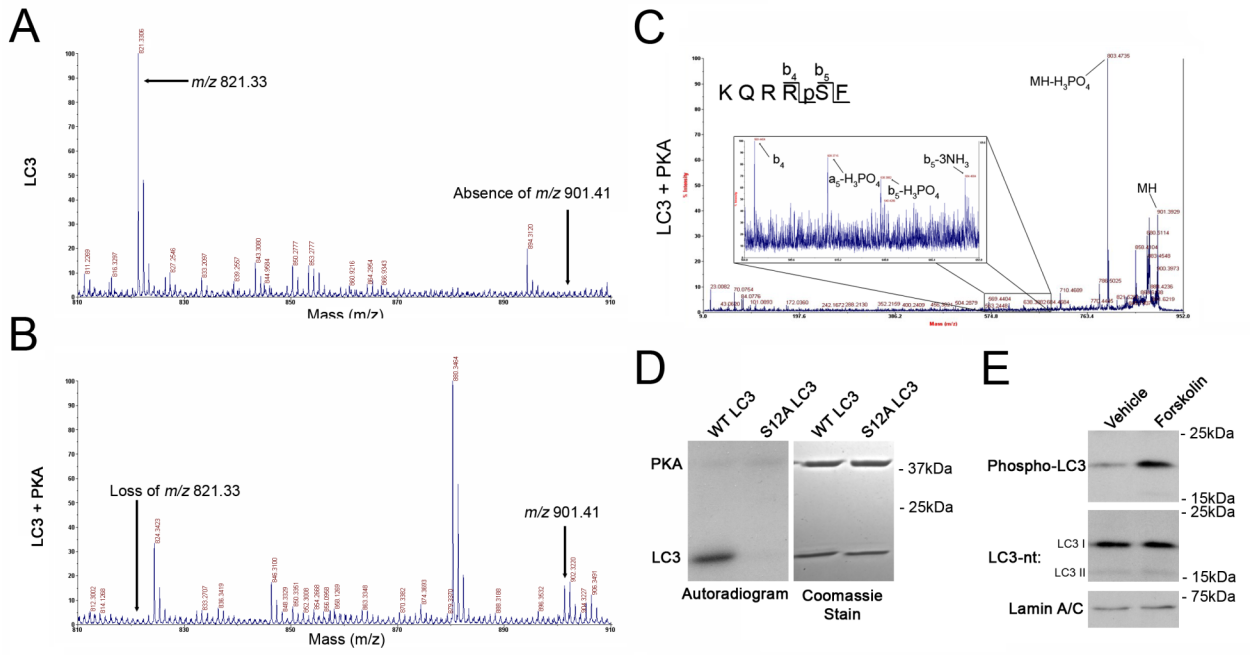


**Figure 12: Identification of PKA phosphorylation site on LC3.**
(A-B) Representative mass spectra from *in vitro* kinase assay with recombinant PKA and LC3. Spectra are representative of 3 independent experiments. A shift from m/z 821.33 to 901.41 was observed in the presence of PKA. (C) Representative spectrum from tandem mass spectrometry analysis of the peak at m/z 901.41. The spectrum is representative of 3 independent experiments. Loss of phosphate peak is indicated as MH-$H_3PO_4$, and ions used for sequence analysis are labeled in the inset. (D) *In vitro* kinase assay with recombinant PKA and LC3-WT or -S12A in the presence of ATP$\gamma^{32}$P. Radioactivity was measured by autoradiography, which represents 1 experiment. (E) Immunoblot from cortical neurons treated with or without forskolin for 1hr. Phospho-LC3 was detected with a custom antibody against the phosphorylated S12 residue. Immunoblots represent 1 experiment.

### 4.3.3 LC3 dephosphorylation is necessary for autophagy induction

To determine whether phosphorylation status is affected by autophagy induction, SH-SY5Y cells were treated with either rapamycin or MPP+ to induce autophagy. The induction of autophagy by either treatment decreased the phosphorylation of LC3 at the S12 residue (Fig. 13A-B). Cotreatment with cAMP prevented this decrease in phosphorylation (Fig. 13B). To determine if LC3 dephosphorylation was sufficient to induce autophagy, the GFP-LC3-S12A mutant was expressed in SH-SY5Y cells and the amount of LC3-II or the number of GFP-LC3 puncta was measured. The S12A phospho-null mutant formed more LC3-II and more LC3 puncta, regardless of the cellular compartment (Fig. 13 C-D). These data suggest that the dephosphorylation of LC3 caused by autophagy induction is sufficient to produce more autophagosomes.

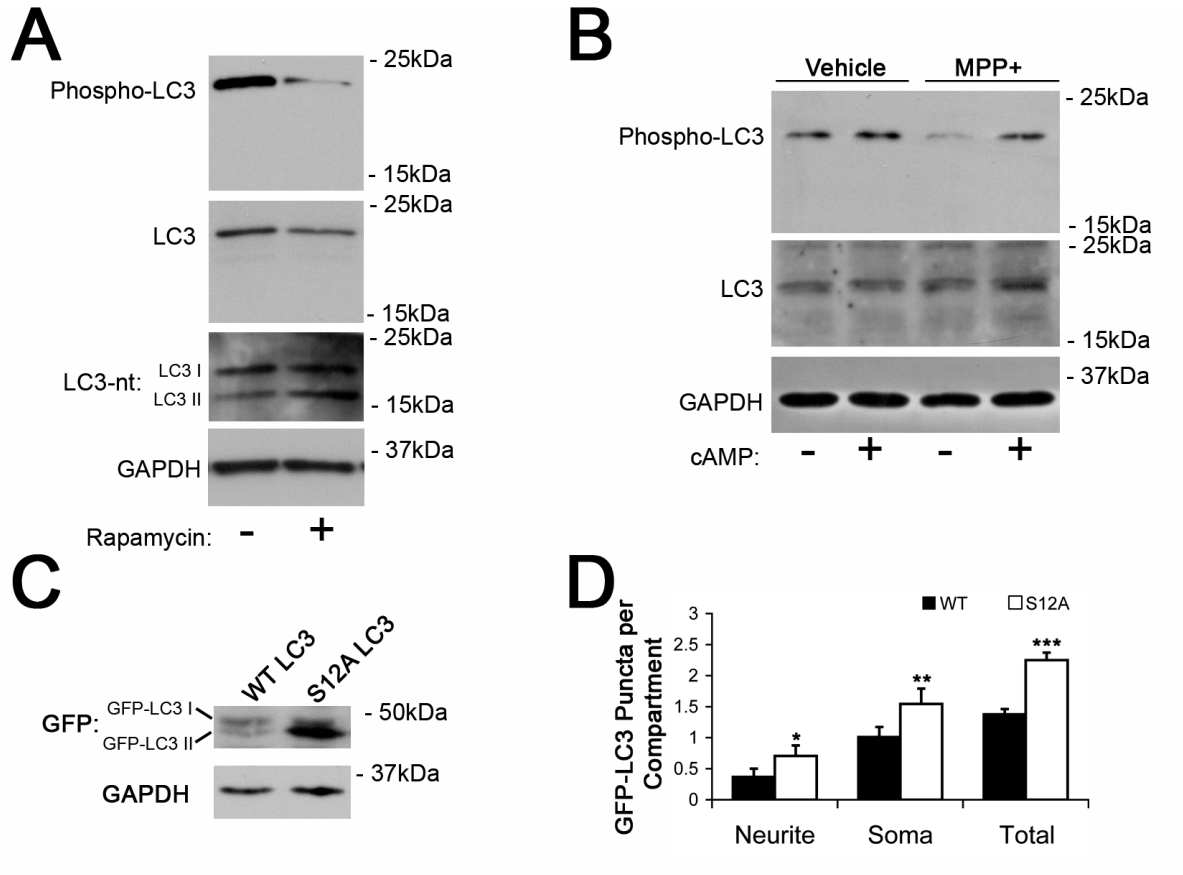


**Figure 13: LC3 is dephosphorylated during autophagy induction.**
(A) Immunoblot from SH-SY5Y cells treated with or without rapamycin for 1hr. Blot was probed for phospho-LC3 and LC3 to determine if autophagy induction affected LC3 phosphorylation. Immunoblots are representative of 2 independent experiments. (B) Immunoblot from SH-SY5Y cells treated with or without MPP+ in the presence or absence of cAMP for 24hrs. Immunoblots represent 1 experiment. (C) Immunoblot from SH-SY5Y cells expressing GFP-LC3-WT or -S12A. Immunoblots represent 3 independent experiments. (D) Quantification of GFP-LC3-WT or -S12A labeled autophagosomes in SH-SY5Y cells and stratified by cellular compartment (mean±SEM; n=100-115 cells/group compiled from 3 independent experiments). *$p<0.05$ vs. WT neurite, *$p<0.05$ vs. WT soma, and ***$p<0.05$ vs. WT total.

### 4.3.4 PKA phosphorylation of LC3 suppresses autophagy and prevents neuronal degeneration

To determine if dephosphorylation of LC3 was necessary for autophagy induction, SH-SY5Y cells expressing the phosphomimetic, GFP-LC3-S12D, were treated with rapamycin. Similar to PKA activation, the S12D mutant formed fewer puncta in the presence of rapamycin (Fig. 14A-

B). Furthermore, in the presence of MPP+ or LRRK2-G2019S, the S12D mutant also formed fewer puncta (Fig. 14C-D), suggesting that PKA regulates pathologic and metabolic induction of autophagy through the phosphorylation of LC3, which is dephosphorylated in order to form autophagosomes.

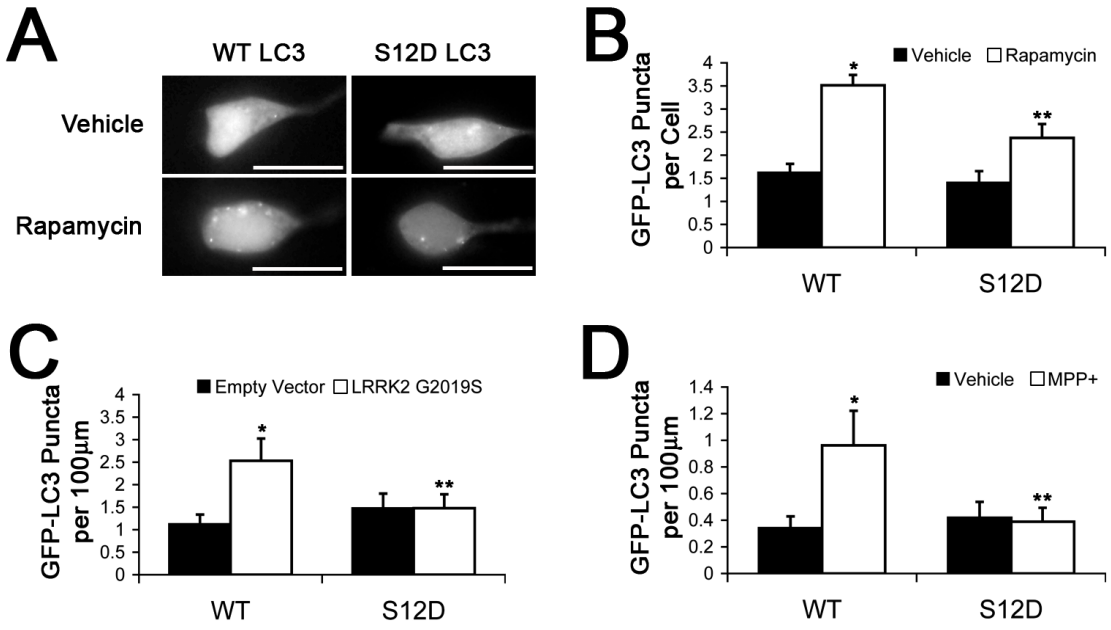


**Figure 14: LC3 phosphorylation suppresses autophagy.**
(A) Representative images from SH-SY5Y cells expressing GFP-LC3-WT or -S12D. Scale bar=20μm. (B) Quantification of GFP-LC3-WT or -S12D labeled autophagosomes in SH-SY5Y cells in the presence or absence of rapamycin (mean±SEM; n=70-80 cells/group compiled from 3 independent experiments). *p<0.05 vs. WT vehicle; **p<0.05 vs. WT rapamycin. (C) Quantification of GFP-LC3-WT or -S12D labeled autophagosomes in SH-SY5Y cells expressing vector or LRRK2 G2019S (mean±SEM; n=110-115 cells/group compiled from 3 independent experiments). *p<0.05 vs. WT vector; **p<0.05 vs. WT LRRK2 G2019S. (D) Quantification of GFP-LC3-WT or -S12D labeled autophagosomes in SH-SY5Y cells treated with or without MPP+ (mean±SEM; n=85-95 cells/group compiled from 3 independent experiments). *p<0.05 vs. WT vehicle; **p<0.05 vs. WT MPP+.

Since autophagy inhibition by PKA activation prevented neurite shortening, the phosphomimetic LC3 was analyzed to determine if it was sufficient to recapitulate the protective effects. Indeed, in SH-SY5Y cells, expression of the LC3-S12D mutant prevented neurite shortening when cells were treated with MPP+ or transfected with LRRK2-G2019S (Fig. 15A-

B). Moreover, LC3-S12D suppressed the neurite shortening and branch simplification in neurons (Fig. 15C-D).

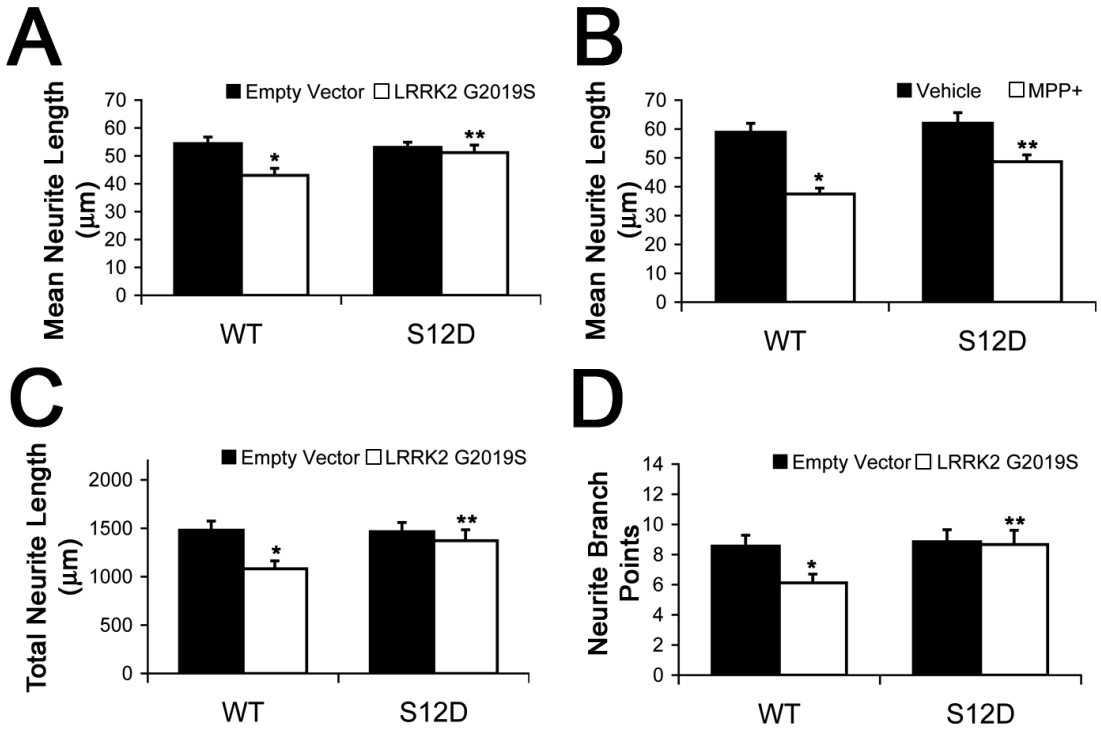


**Figure 15: LC3 phosphorylation reduces neurite shortening.**
(A-B) Quantification of neurite length in SH-SY5Y cells expressing GFP-LC3-WT or -S12D and vector or LRRK2 G2019S or treated with or without MPP+ (mean±SEM; n=110-115 cells/group compiled from 3 independent experiments for A and n=85-95 cells/group compiled from 3 independent experiments for B). *p<0.05 vs. WT vector or vehicle; **p<0.05 vs. WT LRRK2 G2019S or MPP+. (C-D) Quantification of neurite length and branch points in cortical neurons expressing GFP-LC3-WT or -S12D and vector or LRRK2 G2019S mean±SEM; n=30-40 neurons/group compiled from 3 independent experiments). *p<0.05 vs. WT vector; **p<0.05 vs. WT LRRK2 G2019S.

### 4.3.5 The role of phosphorylation on LC3 function

To determine how phosphorylation affected LC3 function, LC3 interacting partners were identified using immunoprecipitations with either GFP-tagged or HA-tagged-LC3 WT, S12A, or S12D followed by mass spectrometry analysis. Although the abundance of most interacting proteins was not effected by phosphorylation status, the interactions between LC3 and CLH1,

AP2B1, HADHA, and HADHB showed a slight reduction in the S12D group as compared to the S12A group (Fig. 16A-B). These results indicate that phosphorylation of LC3 might regulate its interaction with endocytosis machinery (CLH1 and AP2B1) and beta-oxidation/fatty acid degradation in the mitochondria (HADHA and HADHB).

In addition to these differential interactions, many new LC3 interactions were identified (Fig. 16A-B; Table 5). In addition to its roles in microtubule stability and autophagy, these new interactions suggest that LC3 could play a role in membrane trafficking other than autophagy, such as endocytosis or vesicle trafficking (CLH1 and AP2B1), RNA processing, mRNA splicing, and transcriptional regulation (SAFB1, DHX9, PUF60, RBMX, TRA2B, ROA2, THOC4, SFRS9, and SFRS3), fatty acid beta-oxidation (HADHA and HADHB), or even response to DNA damage (PARP1). PUF60 was also found to interact with GFP (data not shown), suggesting that this may interact with the GFP moiety on GFP-LC3 rather than LC3 itself.

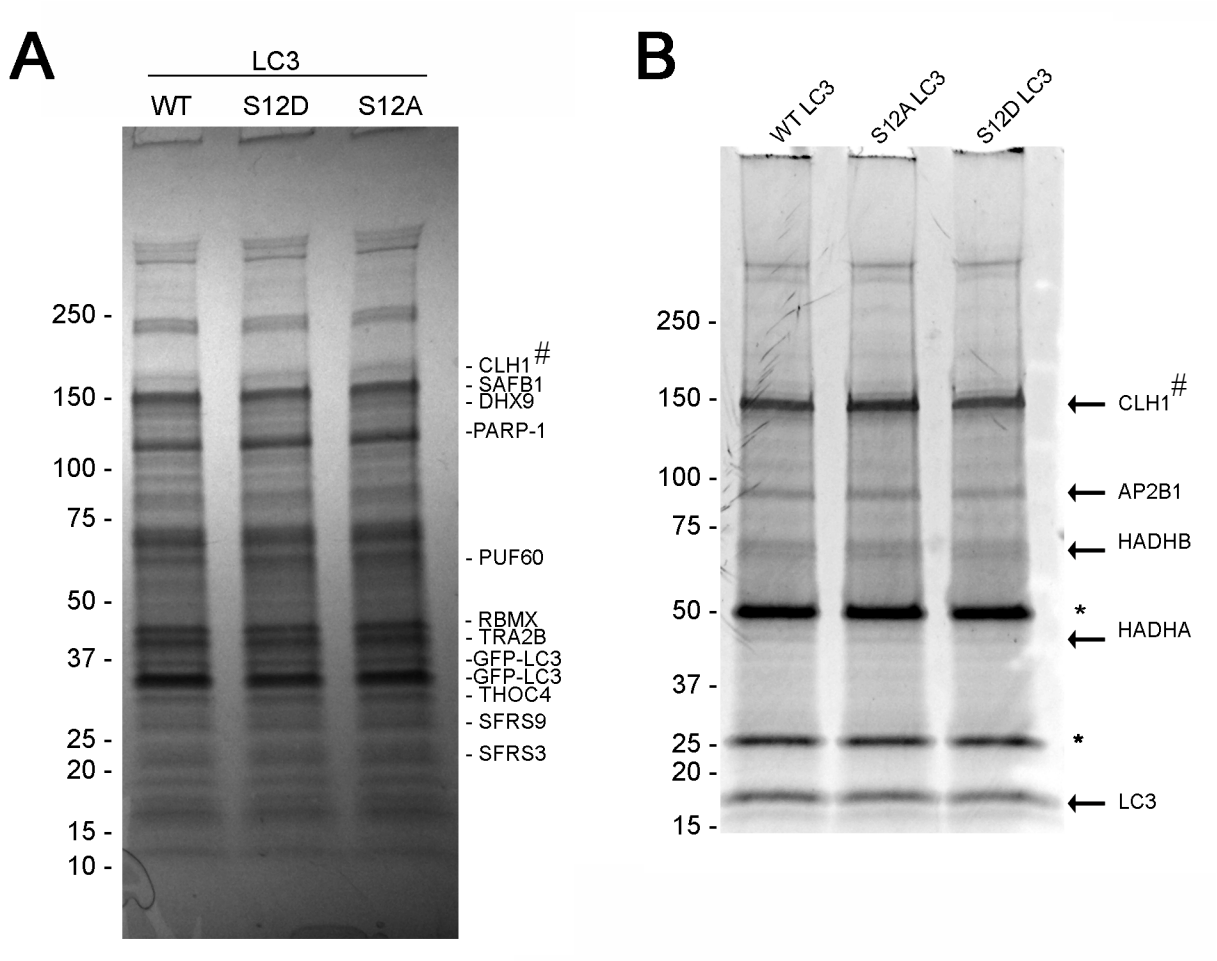


**Figure 16: Identification of new LC3 interacting proteins.**
(A) GFP-LC3-WT, -S12A, and -S12D was immunoprecipitated from HEK293 cells. Interacting proteins were separated by SDS-PAGE and identified by MALDI-TOF-TOF mass spectrometry using the parameters listed in table 3. HNRNPA2B1was identified comigrating with GFP-LC3 and is not indicated on the gel. All proteins listed had Mascot scores >62 ($p<0.05$) and at least 2 unique peptides. (B) HA-LC3-WT, -S12A, and -S12D was immunoprecipitated from HEK293 cells and proteins were analyzed as in (A). All proteins listed, except HADHB, had Mascot scores >62 ($p<0.05$) and at least 2 unique peptides; HADHB had only 1 unique peptide identified. Asterisks denote IgG heavy and light chains; (#) denotes previously identified interactions. Each gel represents 1 experiment.

**Table 5: LC3 Interacting Proteins**

| Gene | Protein | Function |
|---|---|---|
| AP2B1 | Adapter-related protein complex 2 beta 1 | Endocytosis/vesicle traffic |
| CLH1 | Clathrin heavy chain 1 | Endocytosis/vesicle traffic |
| SAFB1 | Scaffold attachment factor B | RNA processing/transcription |
| DHX9 | DEAH (Asp-Glu-Ala-His) box polypeptide 9 | RNA processing/transcription |
| RBMX | RNA binding motif protein, X-linked | RNA processing/transcription |
| TRA2B | Transformer 2 beta homolog | RNA processing/transcription |
| HNRNPA2B1 | Heterogeneous nuclear ribonucleoprotein A2/B1 | RNA processing/transcription |
| THOC4 | THO complex 4 | RNA processing/transcription |
| SFRS9 | Serine/arginine-rich splicing factor 9 | RNA processing/transcription |
| SFRS3 | Serine/arginine-rich splicing factor 3 | RNA processing/transcription |
| PARP1 | Poly (ADP-ribose) polymerase 1 | DNA damage |
| HADHA | Hydroxyacyl-CoA dehydrogenase/3-ketoacyl-CoA thiolase/enoyl-CoA hydratase (trifunctional protein), alpha subunit | Fatty acid beta-oxidation |
| HADHB | Hydroxyacyl-CoA dehydrogenase/3-ketoacyl-CoA thiolase/enoyl-CoA hydratase (trifunctional protein), beta subunit | Fatty acid beta-oxidation |

Although mass spectrometry did not identify tubulin or microtubule-binding proteins as LC3 interactors, LC3 is a microtubule-associated protein[86]. Cortical neurons were treated with forskolin to increase LC3 phosphorylation or rapamycin to decrease LC3 phosphorylation to assess whether phosphorylation altered its ability to bind to microtubules. However, after separating free and polymerized tubulin, there were no discernable differences in LC3 levels between the treatments (Fig. 17), indicating the phosphorylation at S12 does not affect the microtubule binding function of LC3.

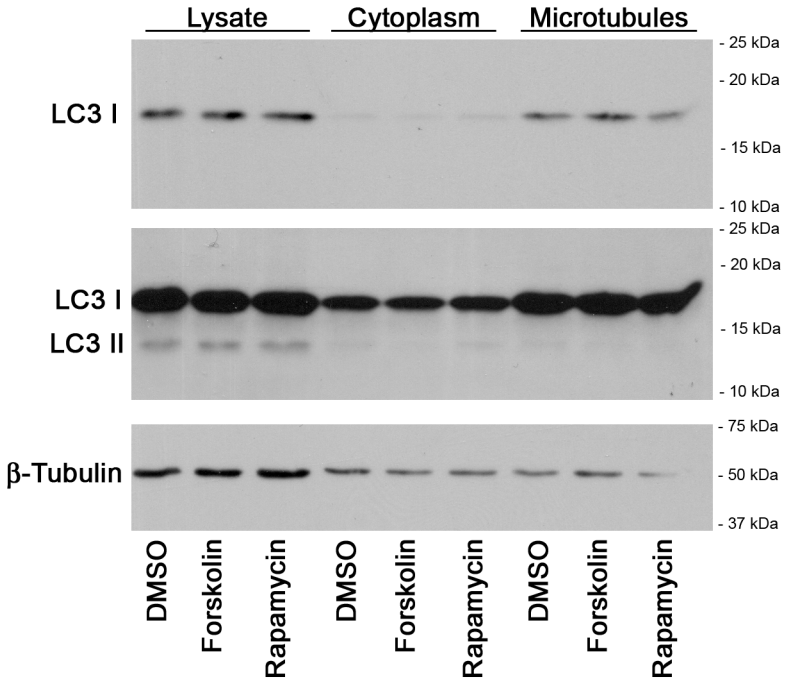


**Figure 17: LC3 phosphorylation does not alter microtubule binding of LC3.**
Cortical neurons were treated with DMSO, forskolin, or rapamycin for 1hr prior to microtubule isolation. Whole cell lysates, cytosplasmic fractions, and microtubule fractions were separated by SDS-PAGE and immunoblotted for LC3. Immunoblots represent 2 independent experiments.

To determine if LC3 phosphorylation altered its interaction with other autophagy proteins not identified by mass spectrometry, immunoprecipitations followed by immunoblotting was used to analyze specific LC3 interactions. Phosphorylation does not affect the interactions between LC3 and Atg3 or Atg7 when autophagy is induced with rapamycin (Fig. 18A). However, the phosphomimetic LC3 showed a reduction in its interaction with p62 during autophagy induction with rapamycin (Fig. 18B). This reduction in LC3-p62 interaction could result in the reduced recruitment of phospho-LC3 to forming autophagosomes around cargo recognized by p62. Together these results suggest that PKA phosphorylation of LC3 may suppress autophagy by altering the cargo selection of autophagosomes, which will be discussed below.

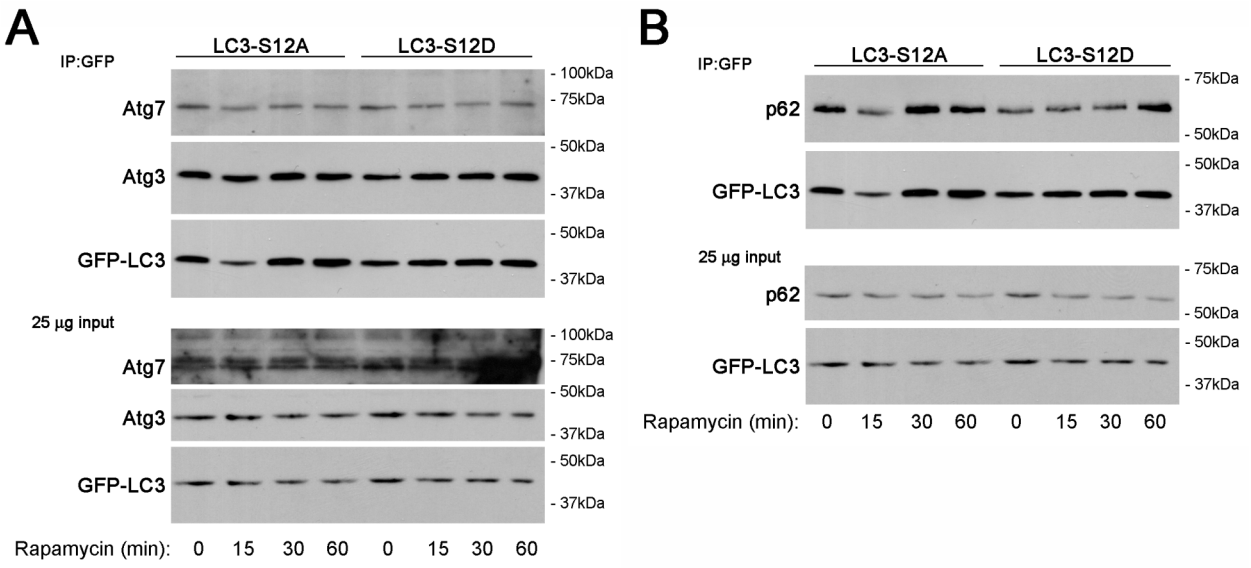


**Figure 18: LC3 phosphorylation perturbs interaction with p62, but not with Atg7 or Atg3.**
(A-B) SH-SY5Y cells expressing GFP-LC3-S12A or -S12D were treated with rapamycin followed by immunoprecipitation of GFP-LC3. Immunoblots were probed for Atg3, Atg7, or p62. Immunoblots represent 1 experiment.

## 4.4 RESTORATION OF CALCIUM HOMEOSTASIS PREVENTS INJURY CAUSED BY MUTANT LRRK2

### 4.4.1 Mutant LRRK2 causes an imbalance in calcium homeostasis

In addition to its effects on mitochondrial homeostasis, mutant LRRK2 also causes an imbalance in calcium buffering (Fig. 19). There were no differences between depolarization-induced calcium influxes in vector- or mutant LRRK2-expressing neurons (Fig. 19A). However, mutant LRRK2-expressing neurons had a delay in calcium clearance after removing the depolarizing stimuli (Fig. 19B-C). To determine if calcium imbalance was upstream or downstream of the mutant LRRK2 elicited decrease in mitochondrial homeostasis, the mitochondrial membrane

potential and mitochondrial content was measured in the presence and absence of BAPTA-AM, an intracellular calcium chelator. BAPTA-AM treatment prevented the reduction in mitochondrial membrane potential, suppressed autophagy, and restored the mitochondrial content to control levels (Fig. 20A-C). Together these results indicate the mutant LRRK2 causes a deficit in calcium clearance that leads to a decrease in mitochondrial polarization and content in the dendrites.

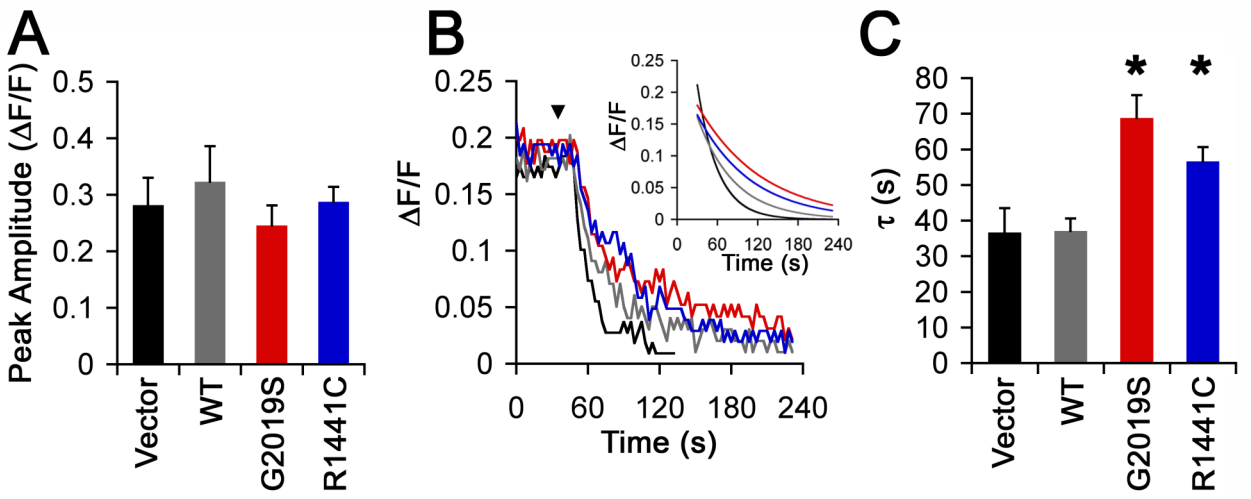


**Figure 19: Mutant LRRK2 induces an imbalance in calcium homeostasis.**
(A) Quantification of calcium influx peak amplitude stimulated with KCl in cortical neurons loaded with Fura2-AM (mean±SEM; n=5-10 neurons/group compiled from at least 3 independent experiments). (B) Representative traces illustrating a delay in calcium clearance in neurons expressing mutant LRRK2. KCl was washed out at the arrowhead. Inset: Monoexponential fits for the calcium decay. (C) Quantification of time constant for calcium decay in neurons expressing vector or LRRK2 after removal of KCl (mean±SEM; n=5-9 neurons/group compiled from at least 3 independent experiments). *p<0.05 vs. vector.

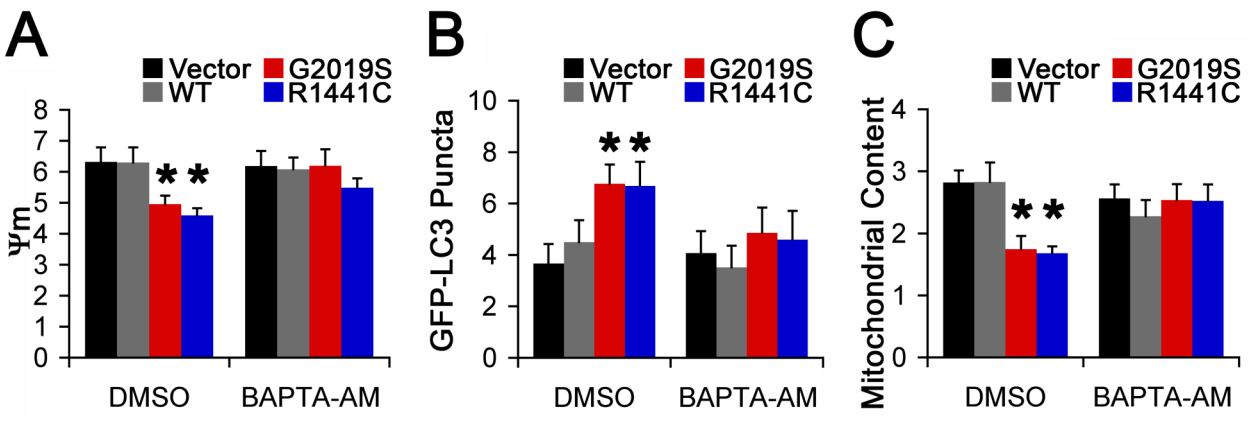


**Figure 20: Calcium chelation prevents mitochondrial depolarization, autophagy, and mitochondrial degradation.**
(A) Quantification of dendritic mitochondrial polarization in cortical neurons in the presence and absence of calcium chelation with BAPTA-AM (mean±SEM; n=15-24 neurons/group compiled from 3 independent experiments). *p<0.05 vs. vector. (B) Quantification of GFP-LC3 labeled autophagosomes in cortical neurons in the presence and absence of BAPTA-AM (mean±SEM; n=13-30 neurons/group compiled from 3 independent experiments). *p<0.05 vs. vector. (C) Quantification of dendritic mitochondrial content in cortical neurons in the presence and absence of BAPTA-AM (mean±SEM; n=19-34 neurons/group compiled from 3 independent experiments). *p<0.05 vs. vector.

### 4.4.2 Voltage-gated calcium channel inhibitors restore calcium homeostasis

Since there are extracellular and intracellular sources of calcium that could be responsible for the elevation in intracellular calcium in neurons expressing mutant LRRK2, EGTA was used to determine which stores were important for the mitochondrial degradation elicited by mutant LRRK2. Similar to chelation of intracellular calcium with BAPTA-AM, EGTA, which is cell impermeable, prevented mitochondrial degradation in mutant LRRK2-expressing cells by chelating extracellular calcium (Fig. 21A). These results indicated that extracellular calcium plays a role in LRRK2-induced mitochondrial degradation.

Voltage-gated calcium channels conduct the majority of calcium influx in the dendrites[8], so this study assessed whether inhibiting these channels would restore calcium homeostasis and abolish mitochondrial degradation caused by mutant LRRK2. Inhibition of the L-type calcium channels with nitrendipine prevented mitochondrial degradation in both the G2019S and R1441C LRRK2 groups; however, inhibition of the N-, P/Q-, and R-type calcium channels with a mixture of $NiCl_2$, ω-agatoxin, and ω-conotoxin provided protection in only the R1441C group (Fig. 21B). Finally, the effects of restoring calcium homeostasis on the neurite shortening elicited by mutant LRRK2 was assessed. Treatment with either BAPTA-AM or nitrendipine attenuated the dendrite shortening in neurons expressing mutant LRRK2 as compared to control (Fig. 21C-D). Similar to its effects on mitochondrial content, the mixture of $NiCl_2$, ω-agatoxin, and ω-conotoxin suppressed the dendrite shortening in the R1441C group, but not the G2019S group (Fig. 21D). Based on these results, restoration of calcium homeostasis prevents mitochondrial dysfunction and degradation and suppresses neurite retraction.

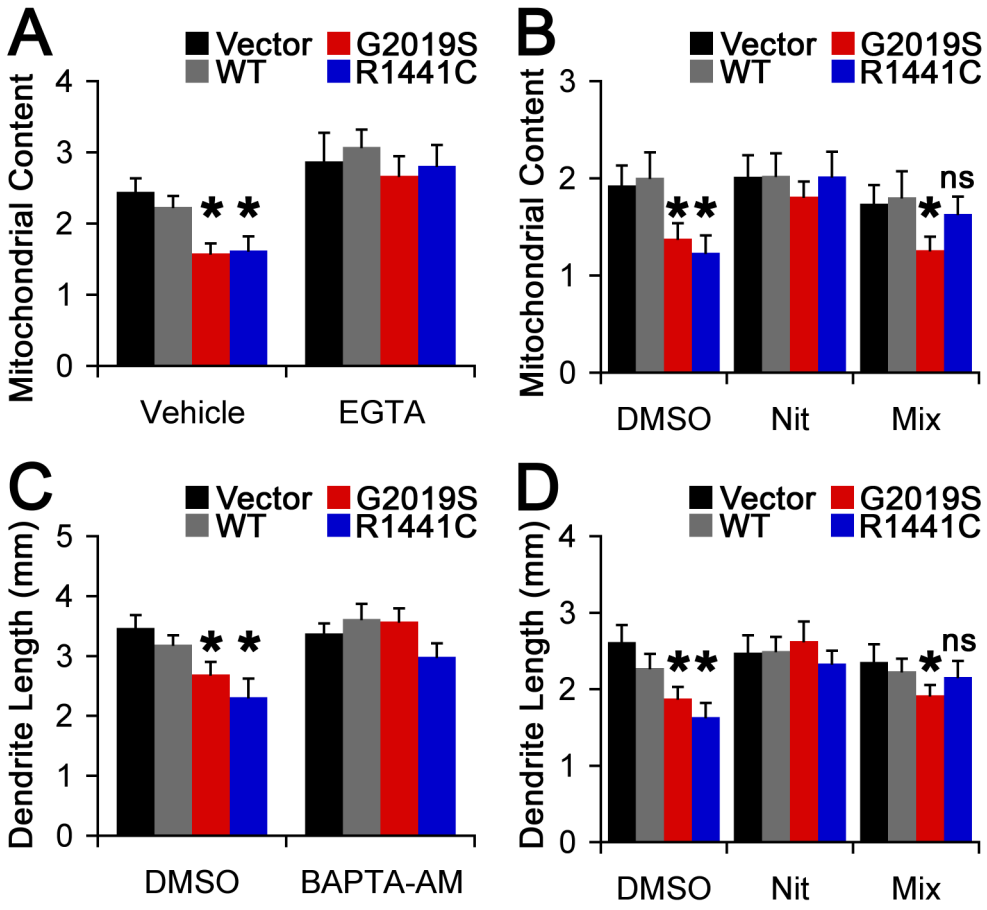


**Figure 21: Calcium channel inhibitors prevent mitochondrial degradation and dendrite shortening.**
(A-B) Quantification of dendritic mitochondrial content in neurons in the presence and absence of EGTA, nitrendipine (Nit), or a mixture of $NiCl_2$, ω-agatoxin, and ω-conotoxin (Mix) (mean±SEM; n=14-31 neurons/group compiled from 3 independent experiments). *p<0.05 vs. vector. (C-D) Quantification of dendrite length in neurons in the presence and absence of BAPTA-AM, nitrendipine, or a mixture of $NiCl_2$, ω-agatoxin, and ω-conotoxin (mean±SEM; n=10-35 neurons/group compiled from 3 independent experiments). *p<0.05 vs. vector.

## 4.5 ELUCIDATION OF A PINK1 SIGNALING NETWORK

### 4.5.1 Identification of PINK1 interacting proteins

As previously mentioned, overexpression of wild type PINK1 suppressed the autophagy, mitochondrial degradation, and neurite shortening induced by mutant LRRK2 expression (Fig. 6A-D). While this could be due to phospho-regulation of LC3 or Drp1, neither of this proteins

are direct substrates for PINK1 (Fig. 7A-B). To identify possible direct mechanisms underlying PINK1 neuroprotection, immunoprecipitations with PINK1-GFP were performed. These results confirmed that PINK1 interacts with Hsp70, Hsp90, and Cdc37 (Fig. 22A-B) as previously reported[87], which validates this method. In addition to these known interacting proteins, ADT2 was also identified as a PINK1 interacting protein (Fig. 22A-B). Interestingly, the engineered kinase-dead mutant K219M and the PD-associated L489P mutant PINK1 displayed increased binding to ADT2 as compared to WT PINK1 (Fig. 22C).

To determine if PINK1 expression altered the phosphorylation status of ADT2, 2D-immunoblotting was performed from HEK 293 cells expressing either GFP or PINK1-GFP. The phosphorylation status of ADT1 and 3 was similar in the cells expressing PINK1-GFP as compared to GFP (Fig. 23A; top and bottom spots). However, there was a shift towards decreased phosphorylation of ADT2 (Fig. 23A; middle set of spots) in the PINK1-GFP sample, suggesting that PINK1 may regulate the phosphorylation status of ADT2 through an indirect mechanism. Interestingly, VDAC, which interacts with ADT2, displayed an increased spot intensity of the more acidic spots and the appearance of a new highly acidic spot in the PINK1-GFP sample, indicative of an increase in phosphorylation (Fig. 23B). This increased phosphorylation is visible in all VDAC isoforms (Fig. 23B; VDAC1: top set of spots, VDAC2: middle set of spots, and VDAC3: bottom set of spots). These results indicate that PINK1 interacts with proteins that comprise the mitochondrial permeability transition pore, suggesting that PINK1 may provide neuroprotection by regulating ion and metabolite flow as one underlying mechanism to support mitochondrial polarization and function.

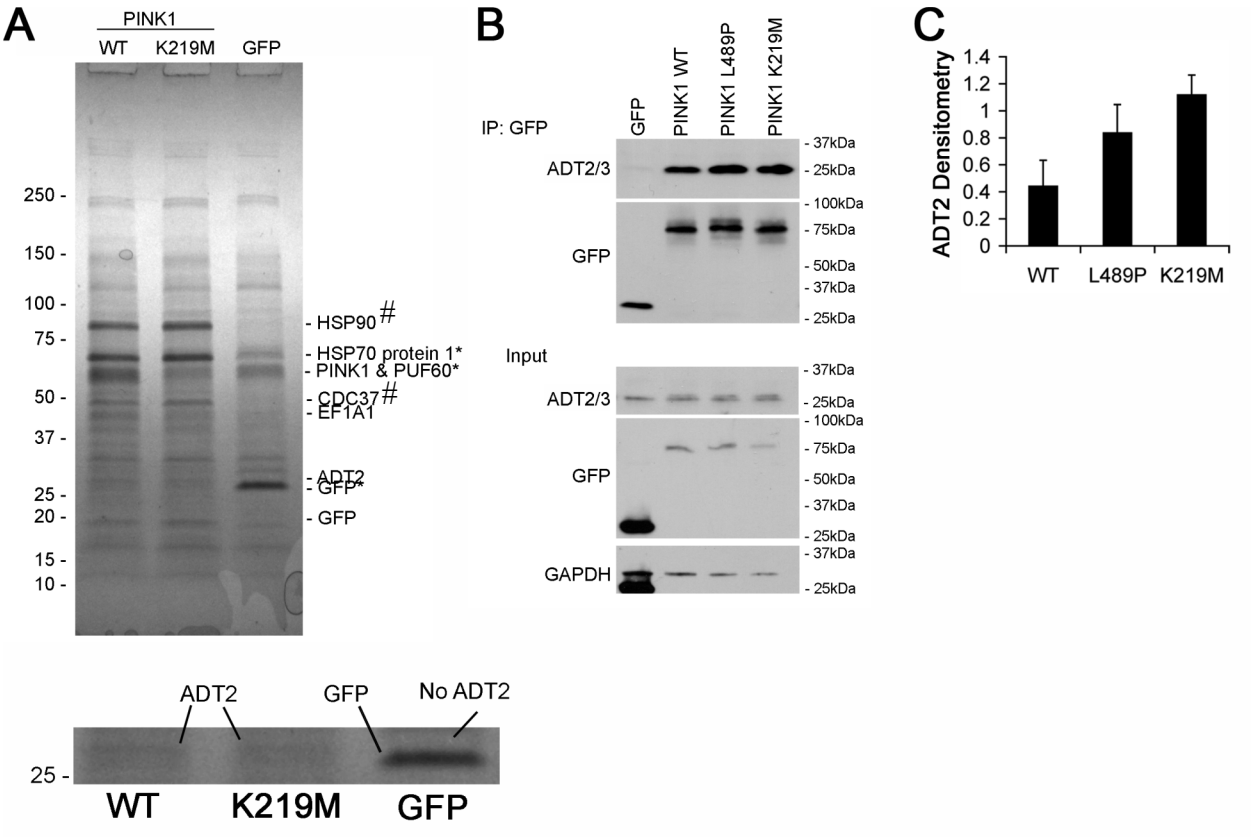


**Figure 22: Identification of new PINK1 interacting proteins.**
(A) PINK1-GFP was immunoprecipitated from HEK293 cells and interacting proteins were separated by SDS-PAGE and identified by MALDI-TOF-TOF mass spectrometry using the parameters listed in table 3. All the listed proteins had Mascot scores >62 ($p<0.05$) and at least 2 unique peptides, with the exception of EF1A1, which had no peptides positively identified. Proteins that were identified in both PINK1 and GFP lanes are marked with an asterisk; (#) denotes previously identified interactions. Gel is representative of 2 independent experiments. Inset: 2X magnified region of gel highlighting the presence of the ADT2 band in the PINK1 WT and K219M lanes only. (B) Immunoblot for PINK1-GFP immunoprecipitated from HEK293 cells to validate the interaction between PINK1 and ADT2. Immunoblots represent 2 independent experiments. (C) Optical density (densitometry) of ADT2 bound to PINK1. Densitometry is the ADT2 density normalized to PINK1 density. Graphical data is mean±SEM with 1 lane/group compiled from 3 independent experiments

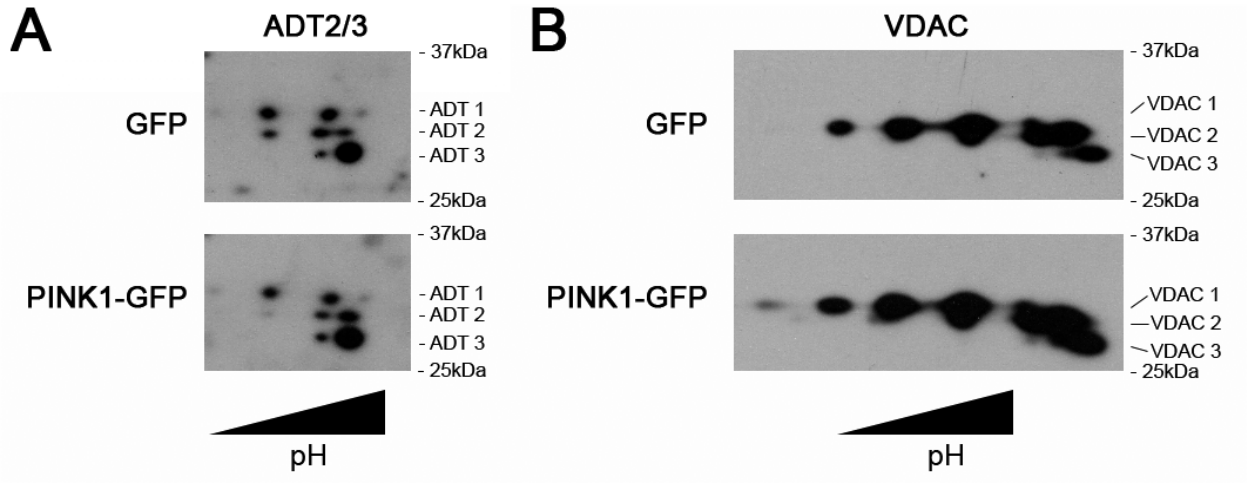


**Figure 23: PINK1 levels regulate VDAC phosphorylation status.**
(A-B) 2-D immunoblots from HEK293 cells expressing GFP or PINK1-GFP. Blots were probed for ADT2/3 or VDAC. Increases in phosphorylation status are indicated as increased staining intensity of more highly acidic spots. Immunoblots represent 1 experiment.

# 5.0 DISCUSSION

## 5.1 MITOCHONDRIAL DYSFUNCTION IN THE LRRK2 MODEL

Mitochondrial dysfunction has been implicated in the pathogenesis of PD for over 20 years. With the discovery of mutations in mitochondrial-targeted proteins, the connection between mitochondrial dysfunction and PD has become even stronger. Interestingly, one of the most common familial PD mutations, the LRRK2 G2019S mutation, occurs in a protein minimally localized with the mitochondria. This study has shown that mutations in LRRK2 do indeed cause mitochondrial dysfunction (Fig. 4). The data suggest that LRRK2 mutants cause a deficit in calcium homeostasis that leads to mitochondrial stress and dysfunction, due to its attempts to buffer the excess intracellular calcium.

Mitochondrial calcium buffering plays an important role in synaptic plasticity, dendrite/axon morphology, and cell survival[8, 84]. The capacity to buffer calcium relies on the electrochemical gradient established across the inner mitochondrial membrane[11]. The mitochondrial polarization derived from this gradient is essential to mitochondrial calcium uptake[11]. Upon calcium uptake, the electrochemical gradient is diminished, resulting in a slight depolarization[11], similar to the observations with mutant LRRK2 expressing cells in this study (Fig. 4). Conversely, mitochondrial depolarization reduces the ability of mitochondria to buffer calcium, leading to elevated intracellular calcium, potentially leading to cell death[8, 10, 11]. This

study indicates that LRRK2 mutants cause an increase in intracellular calcium (Fig. 19), which then leads to mitochondrial depolarization as a compensatory mechanism to buffer the calcium, since calcium chelation prevents the mitochondrial depolarization elicited by mutant LRRK2 (Fig. 20).

In addition to its effects on calcium buffering, which affect mitochondrial homeostasis, LRRK2 also interacts with parkin[88], an E3 ubquitin ligase that regulates mitochondrial degradation. Parkin increases depolarization-induced mitochondrial degradation by autophagy, suggesting that it functions to regulate mitochondrial quality control[85]. Although the effects of LRRK2 mutations on this interaction remain unknown, it is possible that mutations in LRRK2 could perturb the parkin-mediated mitochondrial homeostasis. Interestingly, parkin expression protects against mutations in PINK1 and LRRK2[26, 28, 89], which places parkin downstream of PINK1, which is downstream of LRRK2 according to this study. A reduction in mitochondrial homeostasis could feedback to cause or exacerbate deficits in calcium buffering.

Parkin also regulates synapse stability by enhancing the removal of glutamatergic synapses[90]. Glutamatergic transmission causes influxes of calcium through NMDA and voltage-gated calcium channels during neuronal depolarization[8]. By regulating the number of glutamatergic synapses, parkin may help balance of inhibitory and excitatory inputs, and in doing so could reduce the effects of excitotoxicity due to excessive intracellular calcium. This reduction in calcium influx, either by inhibition of voltage-gated calcium channels in this study (Fig. 20 and 21) or by reducing excitatory synapses, could prevent mitochondrial stress and dysfunction in response to deficits in calcium clearance. This finding suggests that parkin may act through multiple mechanisms to prevent prolonged elevations in calcium and to restore mitochondrial homeostasis in our model as well as others. Furthermore, it is possible that

LRRK2 could regulate glutamatergic synapses through its interaction with parkin, and mutations in LRRK2 could disrupt this function. Overall, mutations in LRRK2 could cause mitochondrial dysfunction through parkin-mediated and parkin-independent mechanisms that disrupt calcium homeostasis preceding degeneration.

Although this study suggests that mutant LRRK2 affects mitochondrial function through an indirect, calcium-mediated mechanism, we cannot rule out direct effects since 10% of LRRK2 localizes to the mitochondria. Since many mitochondrial proteins exist as phosphoproteins and phosphorylation has been shown to regulate mitochondrial proteins such as enzymes in the electron transport chain and the permeability transition pore, it is possible that LRRK2 could directly phosphorylate mitochondrial proteins to alter mitochondrial function. A recent study has even shown that LRRK2 interacts with VDAC and ADT[91]. Direct interactions with these proteins could be an alternative mechanism underlying the mutant LRRK2 induced mitochondria depolarization, since VDAC and ADT regulate the formation of the mitochondrial permeability transition pore that plays a role in mitochondrial depolarization[15]. This could suggest a more direct relationship between PINK1 and LRRK2, whereby they could directly counteract the influence of the other by differentially modifying the same proteins, a theory that will be discussed later.

LRRK2 localization to the mitochondria has been thus far restricted to association with the outer membrane[92]. This finding would place LRRK2 in a position where it could also affect mitochondrial dynamics, such as fusion or fission, which are regulated by proteins associated with the mitochondrial outer membrane and are required for mitophagy[25]. Although LRRK2 mutants did not cause deficits in mitochondrial trafficking (Fig. 2), there was also no compensatory increase in mitochondrial delivery to the neurites, indicating that mutant LRRK2

may perturb compensatory mechanisms for protection such as upregulation of mitochondrial biogenesis. Interestingly, we found that PINK1 might also regulate mitochondrial fusion and fission through the phosphoregulation of Drp1 (Fig. 7A). Without proper fusion/fission events, mitochondrial biogenesis declines and mitochondria cannot be delivered to neurites[93]. Altered mitochondrial dynamics coupled with an increase in mitochondrial degradation would explain the progressive shortening of neurites devoid of mitochondria reporterd in this study. The overexpression of PINK1 may provide compensation for mutations in LRRK2 by enhancing the delivery of mitochondria to dendrites, thus replacing those lost through mitophagy. Mutant LRRK2 could also perturb the compensatory delivery of mitochondria through its effects on microtubule dynamics[42]. Regardless of the mode of mitohcondrial injury (calcium-mediated, direct effects on mitochondrial function, or effects on mitochondrial dynamics), inhibition of autophagic degradation prevents the neurite shortening that follows mitochondria depletion (Fig. 5).

## 5.2 THE ROLE OF LC3 PHOSPHORYLATION

LC3 was initially identified as a microtubule-associated protein that functions to regulate microtubule stability and dynamics[86]. Since microtubules provide support for axons and dendrites in addition to their function as intracellular highways, LC3 phosphorylation could directly play a role in neurite shortening. There were no defects in microtubule binding caused by either the phosphomimetic or phospho-null LC3 mutations (Fig. 17); however, effects of phosphorylation on LC3 binding to MAP1B, which also binds to LC3 and tubulin, were not assessed. Increased interaction with MAP1B has been reported to decrease autophagy levels and

therefore, could be one mechanism through which the phosphorylation of LC3 suppresses autophagy induction[94].

After its initial discovery, LC3 has become widely known as an essential autophagy protein. While its phosphorylation status does not perturb its interaction with Atg3 or Atg7 (Fig. 18), which catalyze the ubiquitin-like reaction that conjugates LC3 to the lipid bilayer of the autophagosome, we did find that phosphorylated LC3 displays a reduced affinity or a delayed recruitment to p62 (Fig. 18). Cargo adaptors such as p62 or NBR1 allow for the recognition of aggregates and ubiquitinated proteins by autophagosomes, aiding in their selective degradation[64, 65]. While autophagosome formation around cargo has only been observed in a few cases, specifically mitophagy[95], it would not be surprising if autophagosomes formed around their cargo rather than phagophores trafficking to their cargo. This theory would allow for high specificity of cargo recognition since the cargo would determine the location and size of the forming autophagosome. As such, the desired cargo would be sequestered with minimal engulfment of non-targeted proteins/organelles. In this scenario, p62 or NBR1 would recruit LC3 to form autophagosomes around their bound cargo, rather than phagophore-bound LC3 recognizing cargo as it engulfs cytoplasmic components. The reduced interaction between phosphorylated LC3 and p62 suggests that this could be a regulatory mechanism for cargo selection that is modulated by PKA.

Besides p62-mediated cargo selection, LC3 can interact directly with cargo since it lines the lumen of the autophagosome. The charge alteration on the N-terminus of LC3 that results from phosphorylation could alter its interactions with other negatively charged cargo, such as phospholipids that comprise the mitochondrion, endoplasmic reticulum, Golgi apparatus, and other membrane-bound organelles. While PKA phosphorylation of LC3 does not suppress basal

autophagy, it prevents stimulus-induced autophagy (Fig. 14). One way that this could happen is through altered targeting of substrates for degradation. By altering cargo recognition, PKA phosphorylation of LC3 could suppress autophagosome formation since there would be a reduction in its interaction with cargo, thus reducing the signal to form autophagosomes. In the case of LRRK2 or even MPP+, this could allow the cell to maintain some level of homeostasis through slightly dysfunctional mitochondria as opposed to losing all mitochondrial function by degrading them. Interestingly, this selective nature of cargo recognition could allow the cell to execute basal autophagy without excessively degrading cytoplasmic components and outstripping the biosynthetic capacities of the cell.

In addition to its known roles in autophagy and microtubule dynamics, new interacting proteins that expand upon the known functions of LC3 have been identified in this study. In addition to its role in membrane trafficking as part of the autophagy pathway, clathrin and AP2 have been identified as new interacting proteins that display differential binding affinity based on LC3 phosphorylation status. Clathrin and AP2 play roles in membrane trafficking in endocytosis and protein transport from the Golgi apparatus[96, 97]. This interaction between clathrin, AP2, and LC3 raises at least three intriguing possibilities. First, this interaction could be one mechanism through which autophagosomes acquire lipids for the expansion of autophagosomes. Clathrin-coated pits form during endocytosis to pinch off portions of the plasma membrane[97]. The recent observation that autophagosomes can utilize plasma membrane[98] as one source of lipids for autophagosomes supports this theory where endosomal machinery can interface with autophagy machinery to generate autophagosomes from plasma membrane lipids.

Second, LC3 could interact with clathrin or AP2 to mediate autophagocytosis of endosomes or even intracellular vesicles. Numerous studies have observed the formation of

multivesicular bodies during autophagy induction[99]. Multivesicular bodies contain many membrane-bound vacuoles within an endosome, which arise due to the engulfment of vesicles and other endosomes[99]. Although further investigation is required, the interaction between LC3 and clathrin could underlie the formation of these multivesicular bodies or the interactions between multivesicular bodies and autophagosomes as yet another link between endocytosis and autophagy.

Finally, these interactions could imply that LC3 plays a role in membrane trafficking outside of autophagy. The membrane extension, curvature, closure, and tethering functions attributed to LC3 could easily be co-opted between multiple membrane trafficking systems. Having one protein involved in multiple membrane trafficking pathways could allow the cell to integrate the regulations of these pathways via post-translational modifications for example. Sequestered cargo during endocytosis could then be directly targeted for degradation rather than having to be processed by the recycling endosome.

Similar to the interactions between LC3 and clathrin or AP2, phosphorylation status of LC3 also affects the interaction between LC3 and members of the fatty acid beta-oxidation pathway, HADHA and HADHB (Fig. 16). These enzymes are located within the mitochondria or cytoplasm and regulate the beta-oxidation of fatty acids[100, 101]. The discovery of this interaction suggests that LC3 could interface with machinery that regulates lipid stores to be utilized for autophagosome formation. While additional studies are required, LC3 through its interaction with HADHA and HADHB could integrate cellular energy requirements that would induce autophagy with the beta-oxidation machinery to generate additional ATP from fatty acid degradation. One could hypothesize that LC3 could deliver either beta-oxidation machinery to fatty acid in the lysosome or vice versa. This would allow for the degradation of lipids, which

accumulate in lysosomal storage diseases if they are not degraded[71]. Since LC3 is dephosphorylated during autophagy induction and dephosphorylated LC3 interacts more abundantly with HADHA and HADHB, this supports the idea of beta-oxidation involvment/regulation during autophagic degradation. An alternative interpretation is that LC3 interacts with these proteins during mitophagy, which does not require p62 involvement. The reduction in the interaction between the phosphomimetic LC3 and HADHA or HADHB supports the idea that LC3 phosphorylation regulates autophagy through cargo recognition, either directly or through the adapter protein, p62. Furthermore, the observation that LC3 phosphorylation reduces its interaction with p62 and potential lipid sources for autophagosome formation provides a possible mechanism to explain why phosphorylated LC3 forms fewer autophagosomes (Fig. 14).

One of the most intriguing observations is the number of interactions detected between LC3 and RNA- and DNA-binding proteins. Eight of the thirteen newly identified interactors regulate gene expression on the transcriptional or post-transcriptional level (SAFB1, DHX9, RBMX, TRA2B, ROA2, THOC4, SFRS9, and SFRS3). These results suggest that LC3 might play a role in the regulation of gene expression. This could be another mechanism similar to mTOR[59], that allows the cell to balance biosynthesis and degradation through the same protein. While more investigation is required, LC3 does possess a putative nuclear export sequence, providing additional support for this hypothesis.

Many studies have linked autophagy induction to DNA damage, and while the mechanisms are poorly understood, the observation that PARP-1 interacts with LC3 (Fig. 16) and the presence of a putative ATM phosphorylation site (Table 4) provide two interesting ways that DNA damage could interface with the autophagy machinery. Upon single strand or double

strand DNA breaks or DNA base lesions, PARP-1 becomes activated and generates chains of poly-ADP-ribose[102]. It is hypothesized that PARP-1 can also poly-ADP-ribosylate proteins as a signaling mechanism to alter protein function, similar to ubiquitination. While poly-ADP-ribosylation is a relatively new idea to cell signaling, LC3 modification could provide a direct link between autophagy and DNA damage. The generation of poly-ADP-ribose from $NAD^+$ during DNA damage also creates a high-energy demand on the cell[103]. Unsurprisingly, this increased energy demand would induce autophagy, similar to nutrient deprivation, as a means to produce more energy. DNA damage also activates ATM, which then phosphorylates its substrates. Although the mechanism remains to be elucidated, LC3 could be a target of ATM, providing one more link between autophagy and DNA damage. Whether through direct signaling or bioenergetic demands, this interaction suggests yet another new function for LC3 in the regulation of cellular homeostasis.

## 5.3 ALTERNATIVE NEUROPROTECTIVE MECHANISMS FOR PKA

While this study has shown that PKA phosphorylation of LC3 is sufficient to prevent mutant LRRK2-induced neurite shortening, numerous other targets of PKA have been identified. PKA also phosphorylates Atg13 and Atg1 in yeast as an additional mechanism to suppress autophagy[81]. Since mutant LRRK2 induces a non-canonical form of autophagy, it would be interesting to investigate whether PKA phosphorylated Atg13 or Atg1 is able to suppress autophagy and restore neurite length in neurons expressing mutant LRRK2. This could elucidate whether Atg13 or Atg1 regulates canonical and non-canonical autophagy, similar to LC3, or if it only regulates canonical autophagy, similar to beclin-1 and the class III PI3K.

Besides autophagy regulation, PKA also affects mitochondrial biology through transcriptional and post-translational mechanisms[104-106]. PKA phosphorylates CREB, which translocates to the nucleus and mitochondria to increase the transcription of targeted genes[106]. CREB translocation to the nucleus increases the expression of prosurvival factors, such as BDNF[75]. It also coordinates the transcription of mitochondrial and nuclear genes encoding subunits of mitochondrial respiration complexes[106]. A more direct mechanism, however, is the PKA mediated phosphorylation of VDAC[104]. Phosphorylation of VDAC has two known functions: first, it inhibits the release of cytochrome c, preventing apoptosis, and second, it allows for increased mitochondrial sequestration of calcium[104]. Activation of PKA has also been reported to inhibit mitochondrial permeability transition, which results from calcium overload[105].

In addition to mitochondrial function, PKA regulates mitochondrial dynamics through the phosphorylation of Drp1[107, 108]. PKA mediated phosphorylation of Drp1 inhibits mitochondrial fission, allowing for the maintenance of mitochondrial networks, which is thought to increase mitochondrial function[107, 108]. One mechanism underlying this increased mitochondrial function is through the diluting of mutations in the mitochondrial genome or defective proteins. In conjunction with its effects on mitochondrial function, the enhanced maintenance of mitochondrial networks suggests that PKA activation increases the overall health of the population of mitochondria in a cell. By enhancing neuronal survival and mitochondrial function, PKA could restore mitochondrial and calcium homeostasis, which are lost in neurons expressing mutant LRRK2.

While the increase in mitochondrial function induced by PKA activation could increase calcium-buffering capacity, PKA has also been shown to regulate voltage-gated calcium channels and glutamate receptors[79, 109-111]. A majority of studies have found that PKA activation

potentiates calcium influx through n-methyl-d-asparate receptor, as well as the release of calcium via ryanodine receptors on the endoplasmic reticulum[109, 112]. Moreover, PKA phosphorylation of voltage-gated calcium channels enhances the influx of calcium[110, 111]. With the exception of one study using immortalized hypothalamic neurons[113], PKA appears to increase intracellular calcium through a number of different receptors and calcium channels. Together, these studies suggest that it is unlikely that PKA would restore calcium homeostasis by reducing its influx. However, BDNF, a downstream target of PKA, increases the expression of calbindin, which can sequester calcium[114]. Although PKA does not directly suppress increases in intracellular calcium, it could induce compensatory mechanisms, such as increased calbindin expression or mitochondrial function, to enhance the calcium buffering of the cell. Overall, PKA regulation of mitochondrial homeostasis and enhanced calcium buffering could underlie additional mechanisms that complement the suppression of autophagy through LC3 phosphorylation, providing multiple modes of protection against mutant LRRK2 induced degeneration.

## 5.4 MECHANISMS OF PINK1-MEDIATED NEUROPROTECTION

PINK1 deficiency causes mitochondrial dysfunction and fragmentation, increased ROS production, and cell death[25-30]. Overexpression of PINK1 reverses these observations and even protects against $H_2O_2$, MPTP/MPP+, 6-hydroxydopamine, and staurosporine[25, 34, 35]. PINK1 also protects against mutant LRRK2 induced injury (Fig. 6). Part of this protection can be attributed to the ability of PINK1 to restore mitochondrial homeostasis, since mutant LRRK2 causes mitochondrial dysfunction leading to degradation.

In addition, PINK1 levels regulate the phosphorylation status of two proteins, Drp1 and LC3, that play roles in mitochondrial fission and autophagy, which combine during the process of mitophagy (Fig. 7). Although neither protein is a direct target of PINK1, these observations agree with previous studies that PINK1 enhances mitochondrial networks and suppresses autophagy. There are two possible interpretations of these results: 1) PINK1 acts to suppress mitophagy, or 2) PINK1 acts to enhance mitochondrial homeostasis, which reduces the need for mitophagy. The second theory seems to be more applicable since PINK1 overexpression leads to healthy mitochondria concurrent with a reduction in autophagy. If PINK1 solely suppressed autophagy and fission, then the mitochondria would not be degraded and would become unhealthy over time unless PINK1 was directly acting upon the mitochondria. Since the mitochondria do not appear sickly during PINK1 overexpression[25], one would conclude that the reduction in autophagy could be attributed to an increase in mitochondrial homeostasis. Therefore, it would appear that enhanced mitochondrial homeostasis would signal for the cell to suppress fission and autophagy, as indicated by the increase in Drp1 and LC3 phosphorylation. These results indicate that the phospho-regulation of these proteins is downstream of and dependent on, but indirect from PINK1.

Based on the PINK1 interaction data, new interacting proteins have been that regulate mitochondrial function and therefore fit into a model whereby PINK1 affects mitochondrial homeostasis upstream of fission and autophagy machinery. Coupled with a previous finding that LRRK2 interacts with ADT and VDAC[91], the interaction between PINK1, VDAC, and ADT2 raises the possibility of converging substrates for these PD genes. Although further investigation is required, differential phosphorylation by PINK1 and LRRK2 could explain how these proteins oppose each other and how mutations in two different proteins can cause PD. ADT2 is one of

three family members that regulate the uptake of ADP into the matrix and release of ATP into the cytosol[115]. By modulating the levels of mitochondrial ADP, ADT2 can directly affect ATP production. For example, during times of high-energy demand, the exchange of mitochondrial ATP for cytosolic ADP increases to allow for faster production of ATP to meet cellular demands[115]. A deficit in calcium buffering is one instance for elevated energy demand[11]. ATP produced during high levels of intracellular calcium is utilized to extrude or sequester calcium via the calcium ATPases[8]. By binding to and affecting the phosphorylation status of ADT2, PINK1 can modulate ATP production and indirectly, affect calcium buffering and cell death. Since PINK1 status inversely correlated with ADT2 phosphorylation status, this regulatory step must be indirect (Fig. 23).

Although indirect regulation of ADT2 phosphorylation was detected with PINK1 overexpression, an increase in VDAC phosphorylation was observed in PINK1 overexpressing cells (Fig. 23). VDAC is a channel that spans the outer mitochondrial and regulates the conductance of ions and metabolites into and out of the mitochondria[116]. VDAC has been directly implicated in mitochondrial calcium buffering as a calcium selective channel when the pore is closed[12, 116]. Interestingly, VDAC closure allows calcium to enter the mitochondrial, but prevents cytochrome c release[116], suggesting that pore closure could enable mitochondria to sequester more calcium without overload-induced apoptosis. Moreover, phosphorylation of VDAC has been associated with pore closure[104], suggesting that PINK1 induced VDAC phosphorylation could be another mechanism through which it regulates mitochondrial function and calcium homeostasis. Further investigation will be required to determine if PINK1 directly phosphorylates VDAC, and if so, at which site and how this phosphorylation affects VDAC function.

The observations that PINK1 interacts with and/or regulates the phosphorylation status of ADT2 and VDAC indicates that PINK1 could perturb the mitochondrial permeability transition and prevent cell death. In support of this theory, a previous study has shown that PINK1 reduces cytochrome c release in response to apoptotic stimuli[34]. This study suggests that by interacting with two components of the permeability transition pore, ADT2 and VDAC, PINK1 could directly regulate mitochondrial polarization. Through phosphorylation of VDAC, PINK1 could even cause direct pore closure as one mechanism that reduces the release of cytochrome c. Combined with previous studies, these results suggest that PINK1 acts to maintain mitochondrial homeostasis by regulating the flow of ions and metabolites through the mitochondria or by indirectly regulating mitochondrial dynamics (fusion/fission/trafficking) or autophagy. Through its affects at the mitochondria, PINK1 could maintain neuronal homeostasis via roles in calcium buffering and suppressing apoptosis.

## 5.5 PINK1 MUTATIONS AS CAUSE FOR DISEASE: A HYPOTHESIS

PINK1 deficiency in cultured cells results in decreased mitochondrial function, increased ROS production, deficits in calcium buffering, and increased cell death[25-30]. In PINK1$^{-/-}$ mice, the phenotype is less severe. There is no neurodegeneration or changes in mitochondrial content, but the animals display a decrease in mitochondrial function accompanied by a minor deficit in synaptic plasticity and evoked dopamine release[27, 31]. The discrepancies between cell culture and mouse models indicate that PD caused by PINK1 mutations may be more complex than simply loss of function. The lack of a degenerative phenotype in mice could suggest an increase in compensatory mechanisms that is absent in cultured cells. There is currently a dearth of studies

investigating the roles of PINK1 mutations in neurobiology, as all mutations have been assumed to cause loss of PINK1 function. One interesting possibility that has received little attention is whether loss of kinase activity could lead to a dominant negative PINK1, which leads to human disease. This could explain the meager phenotype in PINK1$^{-/-}$ mice; however, re-expression of mutant PINK1 in a PINK1 null background has yet to be reported.

PINK1 levels mediate the phosphorylation of TRAP1, ADT2, and VDAC. While the specific effects of phosphorylation on these proteins have yet to be determined, all three have been implicated in suppressing mitochondrial stress and cell death. Since many PINK1 mutations decrease its kinase activity, one mechanism leading to disease could be the loss of PINK1 regulation of TRAP1, ADT2, and VDAC. Through the phospho-regulation of these proteins, PINK1 is poised to modulate cellular oxidative stress levels via TRAP1 and calcium buffering and metabolism via ADT2 and VDAC. When this regulation is lost due to PINK1 mutations, cells would experience elevated ROS levels, decreased mitochondrial function, deficits in calcium buffering, and increased cell death, as previously reported in PINK1 knockdown studies. While the likelihood that PINK1 has other yet-to-be-identified substrates cannot be dismissed, regulation of TRAP1, ADT2, and VDAC could explain the neuroprotective effects of PINK1 overexpression and the deleterious effects of PINK1 deficiency. Although the mechanisms require further investigation, many lines of evidence support a model in which PINK1 mutations that reduce kinase activity lead to familial PD.

As previously mentioned, another theory is that mutant PINK1 could act as a dominant negative molecule. The observation that patients with a heterozygous mutation in PINK1 have altered mitochondrial membrane potentials, nigrostriatal dysfunction, and are at risk for a late-onset form of PD would support a dominant negative role for this mutation since the mutant is

competing with wild type PINK1 in these patients[117, 118]. Moreover, this study has found that mutant PINK1 binds more heavily to PINK1 interacting proteins via immunoprecipitation (Fig. 22). The engineered kinase dead K219M mutation in PINK1 always interacted more abundantly with interacting proteins as compared to wild type PINK1 (Fig. 22A). Although the effects of the L289P mutation were only evaluated in an immunoprecipitation with ADT2, it would be hypothesized that this mutation would have similar effects on the binding with other proteins. With a 2- to 3-fold increase in binding, PINK1 mutants could efficiently possess a dominant negative role; however, more in depth studies will be required. This possible dominant negative function could perturb intracellular signaling pathways that regulate mitochondrial homeostasis and cellular homeostasis through the disruption of chaperone functions or through the mitochondrial exchange of ATP and ADP. These observations could explain how PINK1 mutations that do not disrupt kinase activity could still cause PD. Moreover, dominant negative function of PINK1 mutants would explain why PINK1$^{-/-}$ and PINK1 knockdown animals show no signs of degeneration[27, 31, 119]. It would not be uncommon for mutations that have different effects at the molecular level to produce similar effects at the cellular level, the variety of mutations in LRRK2 provide just one example. Overall, mutations in PINK1 could cause PD via the dysregulation of mitochondrial homeostasis through aberrant or insufficient regulation of ADT2 or VDAC.

# 6.0 CONCLUSIONS

In conclusion, this project has identified a new pathway linking LRRK2, PINK1, and PKA to the regulation of mitochondrial degradation via autophagy and neurite shortening. Mutations in LRRK2 and PINK1 lead to neuronal injury through converging mechanisms. Mutations in LRRK2 disrupted intracellular calcium homeostasis, which led to mitochondrial dysfunction and degradation by autophagy. Restoration of calcium homeostasis through calcium chelation or inhibition of voltage-gated calcium channels presented an early instance for intervention that prevented mitochondrial dysfunction and degradation and neurite shortening. Mutant PINK1 is hypothesized to cause direct mitochondrial dysfunction through aberrant interactions with ADT2 or VDAC. Direct inhibition of autophagy through PKA-mediated LC3 phosphorylation reduced the neurite shortening. Similarly, expression of wild type PINK1, which enhances mitochondrial homeostasis, prevented the mitochondrial degradation and neurite shortening, potentially downstream of the calcium imbalance. This study indicates that LRRK2, PINK1, and PKA regulate mitochondrial function through distinct, yet converging pathways. Based on these observations, therapeutic interventions aimed at maintaining mitochondrial homeostasis by modulating the autophagy pathway or enhancing calcium buffering represents novel targets for the development of new treatments for PD.

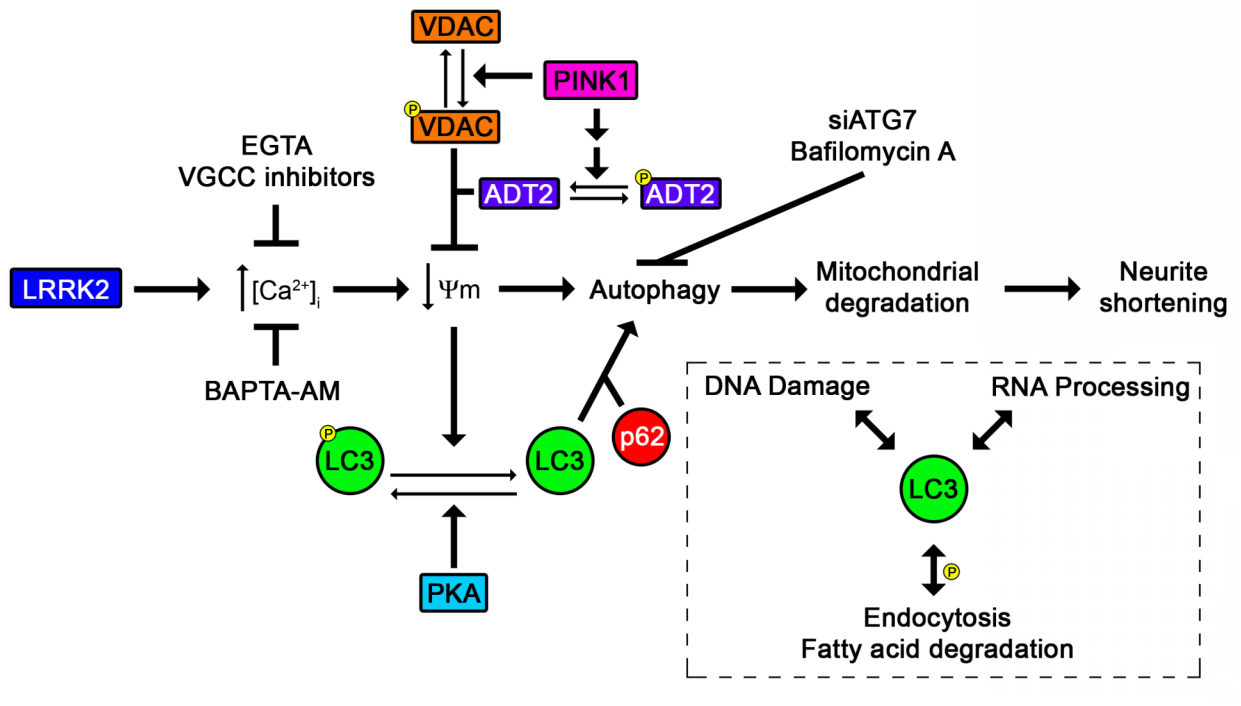


**Figure 24: Summary Figure.**
Mutant LRRK2 causes an increase in intracellular calcium due to a deficit in calcium buffering. As the mitochondrial attempt to buffer the calcium, the lose mitochondrial membrane potential. Depolarized mitochondrial are then degraded through autophagy, and the neurites, devoid of mitochondrial support retract. PKA suppresses the mutant LRRK2 phenotype by inhibiting autophagy through the phosphorylation of LC3, which reduces its interaction with the cargo adapter, p62. Inset: The phosphorylation of LC3 at S12 negatively regulates its interaction with endocytosis and fatty acid degradation machinery. Independent of S12 phosphorylation, LC3 also interacts with the DNA damage pathway, possibly to coordinate the response to cellular stress, and the RNA processing machinery to balance biosynthesis with degradation. PINK1 acts upstream of PKA by regulating mitochondrial function. This study suggests that PINK1 may regulate ADT2 and VDAC to alter mitochondrial function and suppress depolarization.

# 7.0 FUTURE PERSPECTIVES

## 7.1 IDENTIFYING THE LRRK2 SIGNALING PATHWAY

As previously mentioned, LRRK2 has been shown to interact with components of the cytoskeleton, endocytosis proteins, and the proteins that regulate protein synthesis, but determining how mutations in *LRRK2* affect calcium homeostasis requires further investigation. In order to understand how LRRK2 mutants modulate calcium buffering, future studies will utilize immunoprecipitation of LRRK2 to identify binding partners under depolarized and non-depolarized conditions. Similar to the previous studies with PINK1 in this project, non-biased proteomic approaches will be used to identify novel LRRK2 interactors, and targeted strategies will be used to determine if LRRK2 interacts directly with proteins that regulate calcium homeostasis.

Two-dimensional gel analysis in the presence of LRRK2 mutants will be used to identify phospho-proteins regulated by LRRK2. Using this technique, the phosphorylation status of calcium buffering proteins identified through immunoprecipitations will be assessed. In the event that LRRK2 does not directly interact with calcium-buffering proteins, differentially phosphorylated proteins will be identified from 2D gels in the presence or absense of mutant LRRK2. Combined, these non-biased- and targeted-proteomics techniques allow for the

identification of proteins that comprise the LRRK2 signaling pathway, which will provide further insight into PD as well as new proteins to investigate for roles in disease pathogenesis.

These future studies share the pitfalls of using an over-expressed, tagged LRRK2 protein. Although over-expressed wild type LRRK2 will be used as a control for overexpression for all the studies, a possibility exists that the identified interactions may not occur endogenously. To overcome this pitfall, all identified interactions can be verified utilizing a knock-in technique by transfecting LRRK2 mutants or wild type into neurons from $LRRK2^{-/-}$ mice. Since the interaction between most kinases and substrates is very transient, and therefore, difficult to observe, another pitfall could be the lack of identifying LRRK2 substrates via immunoprecipitations. To overcome this problem, future studies will also utilize 2D gel analysis to look for differentially phosphorylated proteins in the presence of mutant LRRK2. After LRRK2 substrates and interacting proteins are identified, the effects of these interactions will be assessed at the cellular and whole animal level with respect to autophagy regulation, mitochondrial homeostasis, and calcium buffering.

Since this project has discovered that *LRRK2* mutations elicit a deficit in calcium buffering, future calcium-imaging studies will investigate the roles of the endoplasmic reticulum, the mitochondria, and plasma membrane ATPases to determine if mutant LRRK2 affects calcium homeostasis by disrupting one of these calcium-buffering mechanisms. The level of calcium in the mitochondria and endoplasmic reticulum will be analyzed in the presence or absence of mutant LRRK2. Determining which compartments become dysfunctional in the presence of mutant LRRK2 will provide a subcellular localization, in which to further probe for LRRK2 substrates. These studies will provide vital information regarding how *LRRK2* mutations directly affect calcium homeostasis and the subsequent neurodegeneration.

## 7.2 UNDERSTANDING THE PINK1 NETWORK

In this project, novel PINK1 interactors have been identified in preliminary experiments. To further validate the interaction between PINK1 and ADT2, future studies will utilize immunoprecipitations for ADT2-GFP followed by immunoblotting for endogenous PINK1. To further determine if ADT2 or VDAC1 are PINK1 substrates, 2D immunoblots will be performed in the presence or absence of PINK1 WT, L489P, or K219M. Future studies will also determine if PINK1 directly phosphorylates either of these proteins. If PINK1 phosphorylates either protein, either directly or indirectly, mass spectrometry and site-directed mutagenesis will be utilized to confirm the identification of the phosphorylation site. Additional studies would investigate the biological functions of these phosphorylation sites on mitochondrial homeostasis, calcium buffering, and protecting from mutant LRRK2-induced neurodegeneration. These studies will investigate the potential PINK1 substrates; furthermore, these studies may uncover the mechanism(s) responsible for PD associated with *PINK1* mutations.

In the event that PINK1 does not phosphorylate these newly identified interactors, bioinformatics will be used to identify potential kinases capable of phosphorylating the identified residues, whose phosphorylation status is modulated by PINK1. In this case, additional studies would be focused on how PINK1 regulates these sites, what other kinases are involved, and how this network affects mitochondrial homeostasis and neurodegeneration.

## 7.3 ELUCIDATING THE ROLE OF LC3 PHOSPHORYLATION

While the preliminary results suggest that LC3 phosphorylation modulates its interaction with endosomal machinery and the autophagy cargo adapter protein, p62, these interactions require further investigation. First, immunoblot confirmation of the interactions is required to better assess the affects of LC3 phosphorylation on these interactions. To further validate and investigate the function of LC3 phosphorylation, future studies will use site-directed mutagenesis to disrupt these interactions to determine the biological effects of LC3-p62, -clathrin, and -AP2 interactions. Future studies should also aim at determining which species of LC3, LC3-I or LC3-II, binds to the identified binding partners since this information would greatly impact the understanding of LC3 function in each of these interactions. For example, does the endosomal machinery interaction with LC3 as a component of the autophagy pathway or as a component of the cytoskeleton? This data could provide insight into why LC3 phosphorylation reduces its incorporation into autophagosomes and provides protection against toxin and genetic models of PD.

In addition to p62, other autophagy adapter proteins, such as NBR1, should be investigated to determine whether phosphorylation of LC3 modulates all interactions with adapter proteins, or if it provides more specific regulation of LC3 function. These data would answer the question of whether LC3 phosphorylation suppresses autophagy induction or simply alters cargo recognition. Furthermore, LC3 phosphorylation appears to cause variable shifts when comparing either tumor cells to normal cells or human cells to murine cells. This is evident in the increase in apparent molecular weight of phospho-LC3 (~20kDa; greater than LC3-I) in human tumor cell lines versus murine neurons (~16kDa; identical to LC3-I). Additional studies will investigate why this apparent size difference exists by probing for additional post-

translational modifications that may cause this shift in molecular weight. Isoform differences between the cell types will also be investigated to determine if differential expression of isoforms could be the underlying reason for this shift in the apparent molecular weight, since LC3a and b have been detected at ~16kDa and LC3c at ~18kDa. These studies should provide more insight in the regulation of autophagy by LC3, focusing on the post-translational modification and protein-protein interactions that regulate this key autophagy protein.

In summary, the future studies will extend the preliminary discoveries of this project to elucidate the cellular and molecular mechanisms underlying neurodegeneration caused by *LRRK2* mutations. Furthermore, they will investigate the PINK1 signaling pathway to understand how it modulates mitochondrial homeostasis and function and to identify downstream targets that may present points for therapeutic intervention. Finally, the effects of post-translational modifications on LC3 will be further investigated. The findings from these studies will illustrate how LC3 is regulated and how it regulates intracellular events that affect neurodegeneration both within and beyond the autophagy pathway. The preliminary findings reported from this project will provide a basis for the discovery of the molecular mechanisms underlying parkinsonian neurodegeneration as well as potential therapeutic targets to better treat PD.

## BIBLIOGRAPHY


1. Parkinson, J. An essay on the shaking palsy. 1817. *The Journal of neuropsychiatry and clinical neurosciences* **14**, 223-236; discussion 222 (2002).
2. Mitchell, S.L., Kiely, D.K., Kiel, D.P. & Lipsitz, L.A. The epidemiology, clinical characteristics, and natural history of older nursing home residents with a diagnosis of Parkinson's disease. *Journal of the American Geriatrics Society* **44**, 394-399 (1996).
3. Toulouse, A. & Sullivan, A.M. Progress in Parkinson's disease-where do we stand? *Progress in neurobiology* **85**, 376-392 (2008).
4. Galvan, A. & Wichmann, T. Pathophysiology of parkinsonism. *Clin Neurophysiol* **119**, 1459-1474 (2008).
5. Young, R. Update on Parkinson's disease. *American family physician* **59**, 2155-2167, 2169-2170 (1999).
6. Braak, H.*, et al.* Stanley Fahn Lecture 2005: The staging procedure for the inclusion body pathology associated with sporadic Parkinson's disease reconsidered. *Mov Disord* **21**, 2042-2051 (2006).
7. Lin, M.T. & Beal, M.F. Mitochondrial dysfunction and oxidative stress in neurodegenerative diseases. *Nature* **443**, 787-795 (2006).
8. Mattson, M.P. Calcium and neurodegeneration. *Aging cell* **6**, 337-350 (2007).
9. Rubinsztein, D.C. The roles of intracellular protein-degradation pathways in neurodegeneration. *Nature* **443**, 780-786 (2006).
10. Nicholls, D.G. & Budd, S.L. Mitochondria and neuronal survival. *Physiological reviews* **80**, 315-360 (2000).
11. Nicholls, D.G. Mitochondrial calcium function and dysfunction in the central nervous system. *Biochimica et biophysica acta* **1787**, 1416-1424 (2009).
12. Rapizzi, E.*, et al.* Recombinant expression of the voltage-dependent anion channel enhances the transfer of Ca2+ microdomains to mitochondria. *The Journal of cell biology* **159**, 613-624 (2002).
13. De Stefani, D., Raffaello, A., Teardo, E., Szabo, I. & Rizzuto, R. A forty-kilodalton protein of the inner membrane is the mitochondrial calcium uniporter. *Nature* (2011).
14. Lemasters, J.J. & Ramshesh, V.K. Imaging of mitochondrial polarization and depolarization with cationic fluorophores. *Methods in cell biology* **80**, 283-295 (2007).
15. Lemasters, J.J., Theruvath, T.P., Zhong, Z. & Nieminen, A.L. Mitochondrial calcium and the permeability transition in cell death. *Biochimica et biophysica acta* **1787**, 1395-1401 (2009).
16. Liang, C.L., Wang, T.T., Luby-Phelps, K. & German, D.C. Mitochondria mass is low in mouse substantia nigra dopamine neurons: implications for Parkinson's disease. *Experimental neurology* **203**, 370-380 (2007).

17. Foehring, R.C., Zhang, X.F., Lee, J.C. & Callaway, J.C. Endogenous calcium buffering capacity of substantia nigral dopamine neurons. *Journal of neurophysiology* **102**, 2326-2333 (2009).
18. Yamada, T., McGeer, P.L., Baimbridge, K.G. & McGeer, E.G. Relative sparing in Parkinson's disease of substantia nigra dopamine neurons containing calbindin-D28K. *Brain research* **526**, 303-307 (1990).
19. Silvestri, L.*, et al.* Mitochondrial import and enzymatic activity of PINK1 mutants associated to recessive parkinsonism. *Human molecular genetics* **14**, 3477-3492 (2005).
20. Hatano, Y.*, et al.* Novel PINK1 mutations in early-onset parkinsonism. *Annals of neurology* **56**, 424-427 (2004).
21. Rohe, C.F.*, et al.* Homozygous PINK1 C-terminus mutation causing early-onset parkinsonism. *Annals of neurology* **56**, 427-431 (2004).
22. Valente, E.M.*, et al.* Hereditary early-onset Parkinson's disease caused by mutations in PINK1. *Science (New York, N.Y* **304**, 1158-1160 (2004).
23. Valente, E.M.*, et al.* PINK1 mutations are associated with sporadic early-onset parkinsonism. *Annals of neurology* **56**, 336-341 (2004).
24. Cookson, M.R. The biochemistry of Parkinson's disease. *Annual review of biochemistry* **74**, 29-52 (2005).
25. Dagda, R.K.*, et al.* Loss of PINK1 function promotes mitophagy through effects on oxidative stress and mitochondrial fission. *The Journal of biological chemistry* **284**, 13843-13855 (2009).
26. Clark, I.E.*, et al.* Drosophila pink1 is required for mitochondrial function and interacts genetically with parkin. *Nature* **441**, 1162-1166 (2006).
27. Gautier, C.A., Kitada, T. & Shen, J. Loss of PINK1 causes mitochondrial functional defects and increased sensitivity to oxidative stress. *Proceedings of the National Academy of Sciences of the United States of America* **105**, 11364-11369 (2008).
28. Park, J.*, et al.* Mitochondrial dysfunction in Drosophila PINK1 mutants is complemented by parkin. *Nature* **441**, 1157-1161 (2006).
29. Poole, A.C.*, et al.* The PINK1/Parkin pathway regulates mitochondrial morphology. *Proceedings of the National Academy of Sciences of the United States of America* **105**, 1638-1643 (2008).
30. Gandhi, S.*, et al.* PINK1-associated Parkinson's disease is caused by neuronal vulnerability to calcium-induced cell death. *Molecular cell* **33**, 627-638 (2009).
31. Kitada, T.*, et al.* Impaired dopamine release and synaptic plasticity in the striatum of PINK1-deficient mice. *Proceedings of the National Academy of Sciences of the United States of America* **104**, 11441-11446 (2007).
32. Pridgeon, J.W., Olzmann, J.A., Chin, L.S. & Li, L. PINK1 protects against oxidative stress by phosphorylating mitochondrial chaperone TRAP1. *PLoS biology* **5**, e172 (2007).
33. Weihofen, A., Thomas, K.J., Ostaszewski, B.L., Cookson, M.R. & Selkoe, D.J. Pink1 forms a multiprotein complex with Miro and Milton, linking Pink1 function to mitochondrial trafficking. *Biochemistry* **48**, 2045-2052 (2009).
34. Petit, A.*, et al.* Wild-type PINK1 prevents basal and induced neuronal apoptosis, a protective effect abrogated by Parkinson disease-related mutations. *The Journal of biological chemistry* **280**, 34025-34032 (2005).

35. Haque, M.E., *et al.* Cytoplasmic Pink1 activity protects neurons from dopaminergic neurotoxin MPTP. *Proceedings of the National Academy of Sciences of the United States of America* **105**, 1716-1721 (2008).
36. Cherra, S.J., 3rd, Dagda, R.K., Tandon, A. & Chu, C.T. Mitochondrial autophagy as a compensatory response to PINK1 deficiency. *Autophagy* **5**, 1213-1214 (2009).
37. Paisan-Ruiz, C., *et al.* Cloning of the gene containing mutations that cause PARK8-linked Parkinson's disease. *Neuron* **44**, 595-600 (2004).
38. Zimprich, A., *et al.* Mutations in LRRK2 cause autosomal-dominant parkinsonism with pleomorphic pathology. *Neuron* **44**, 601-607 (2004).
39. Alegre-Abarrategui, J., *et al.* LRRK2 regulates autophagic activity and localizes to specific membrane microdomains in a novel human genomic reporter cellular model. *Human molecular genetics* **18**, 4022-4034 (2009).
40. Cherra, S.J., 3rd, *et al.* Regulation of the autophagy protein LC3 by phosphorylation. *The Journal of cell biology* **190**, 533-539 (2010).
41. Plowey, E.D., Cherra, S.J., 3rd, Liu, Y.J. & Chu, C.T. Role of autophagy in G2019S-LRRK2-associated neurite shortening in differentiated SH-SY5Y cells. *Journal of neurochemistry* **105**, 1048-1056 (2008).
42. Gillardon, F. Leucine-rich repeat kinase 2 phosphorylates brain tubulin-beta isoforms and modulates microtubule stability--a point of convergence in parkinsonian neurodegeneration? *Journal of neurochemistry* **110**, 1514-1522 (2009).
43. Jaleel, M., *et al.* LRRK2 phosphorylates moesin at threonine-558: characterization of how Parkinson's disease mutants affect kinase activity. *The Biochemical journal* **405**, 307-317 (2007).
44. Parisiadou, L., *et al.* Phosphorylation of ezrin/radixin/moesin proteins by LRRK2 promotes the rearrangement of actin cytoskeleton in neuronal morphogenesis. *J Neurosci* **29**, 13971-13980 (2009).
45. Gehrke, S., Imai, Y., Sokol, N. & Lu, B. Pathogenic LRRK2 negatively regulates microRNA-mediated translational repression. *Nature* **466**, 637-641 (2010).
46. Imai, Y., *et al.* Phosphorylation of 4E-BP by LRRK2 affects the maintenance of dopaminergic neurons in Drosophila. *The EMBO journal* **27**, 2432-2443 (2008).
47. Piccoli, G., *et al.* LRRK2 controls synaptic vesicle storage and mobilization within the recycling pool. *J Neurosci* **31**, 2225-2237 (2011).
48. Shin, N., *et al.* LRRK2 regulates synaptic vesicle endocytosis. *Experimental cell research* **314**, 2055-2065 (2008).
49. Klionsky, D.J. & Emr, S.D. Autophagy as a regulated pathway of cellular degradation. *Science (New York, N.Y* **290**, 1717-1721 (2000).
50. Clark, S.L., Jr. Cellular differentiation in the kidneys of newborn mice studies with the electron microscope. *The Journal of biophysical and biochemical cytology* **3**, 349-362 (1957).
51. Melendez, A., *et al.* Autophagy genes are essential for dauer development and life-span extension in C. elegans. *Science (New York, N.Y* **301**, 1387-1391 (2003).
52. Cherra, S.J. & Chu, C.T. Autophagy in neuroprotection and neurodegeneration: A question of balance. *Future neurology* **3**, 309-323 (2008).
53. Essick, E.E. & Sam, F. Oxidative stress and autophagy in cardiac disease, neurological disorders, aging and cancer. *Oxidative medicine and cellular longevity* **3**, 168-177 (2010).

54. Huett, A. & Xavier, R.J. Autophagy at the gut interface: mucosal responses to stress and the consequences for inflammatory bowel diseases. *Inflammatory bowel diseases* **16**, 152-174 (2009).
55. Deretic, V. Autophagy in immunity and cell-autonomous defense against intracellular microbes. *Immunological reviews* **240**, 92-104 (2011).
56. Kirkin, V. & Dikic, I. Ubiquitin networks in cancer. *Current opinion in genetics & development* **21**, 21-28 (2011).
57. Cuervo, A.M. & Dice, J.F. A receptor for the selective uptake and degradation of proteins by lysosomes. *Science (New York, N.Y* **273**, 501-503 (1996).
58. Kaushik, S., Massey, A.C., Mizushima, N. & Cuervo, A.M. Constitutive activation of chaperone-mediated autophagy in cells with impaired macroautophagy. *Molecular biology of the cell* **19**, 2179-2192 (2008).
59. Cherra, S.J., 3rd, Dagda, R.K. & Chu, C.T. Review: autophagy and neurodegeneration: survival at a cost? *Neuropathology and applied neurobiology* **36**, 125-132 (2010).
60. Codogno, P. & Meijer, A.J. Autophagy and signaling: their role in cell survival and cell death. *Cell death and differentiation* **12 Suppl 2**, 1509-1518 (2005).
61. He, C., Baba, M. & Klionsky, D.J. Double duty of Atg9 self-association in autophagosome biogenesis. *Autophagy* **5**, 385-387 (2009).
62. Ohsumi, Y. Molecular dissection of autophagy: two ubiquitin-like systems. *Nature reviews* **2**, 211-216 (2001).
63. He, C. & Klionsky, D.J. Regulation mechanisms and signaling pathways of autophagy. *Annual review of genetics* **43**, 67-93 (2009).
64. Kirkin, V.*, et al.* A role for NBR1 in autophagosomal degradation of ubiquitinated substrates. *Molecular cell* **33**, 505-516 (2009).
65. Pankiv, S.*, et al.* p62/SQSTM1 binds directly to Atg8/LC3 to facilitate degradation of ubiquitinated protein aggregates by autophagy. *The Journal of biological chemistry* **282**, 24131-24145 (2007).
66. Yamamoto, A.*, et al.* Bafilomycin A1 prevents maturation of autophagic vacuoles by inhibiting fusion between autophagosomes and lysosomes in rat hepatoma cell line, H-4-II-E cells. *Cell structure and function* **23**, 33-42 (1998).
67. Hara, T.*, et al.* Suppression of basal autophagy in neural cells causes neurodegenerative disease in mice. *Nature* **441**, 885-889 (2006).
68. Komatsu, M.*, et al.* Loss of autophagy in the central nervous system causes neurodegeneration in mice. *Nature* **441**, 880-884 (2006).
69. Pickford, F.*, et al.* The autophagy-related protein beclin 1 shows reduced expression in early Alzheimer disease and regulates amyloid beta accumulation in mice. *The Journal of clinical investigation* **118**, 2190-2199 (2008).
70. Shibata, M.*, et al.* Regulation of intracellular accumulation of mutant Huntingtin by Beclin 1. *The Journal of biological chemistry* **281**, 14474-14485 (2006).
71. Kiselyov, K., Jennigs, J.J., Jr., Rbaibi, Y. & Chu, C.T. Autophagy, mitochondria and cell death in lysosomal storage diseases. *Autophagy* **3**, 259-262 (2007).
72. Mitchison, H.M., Lim, M.J. & Cooper, J.D. Selectivity and types of cell death in the neuronal ceroid lipofuscinoses. *Brain pathology (Zurich, Switzerland)* **14**, 86-96 (2004).
73. Nixon, R.A. Autophagy, amyloidogenesis and Alzheimer disease. *Journal of cell science* **120**, 4081-4091 (2007).

74. Zhu, J.H., *et al.* Regulation of autophagy by extracellular signal-regulated protein kinases during 1-methyl-4-phenylpyridinium-induced cell death. *The American journal of pathology* **170**, 75-86 (2007).
75. Chalovich, E.M., Zhu, J.H., Caltagarone, J., Bowser, R. & Chu, C.T. Functional repression of cAMP response element in 6-hydroxydopamine-treated neuronal cells. *The Journal of biological chemistry* **281**, 17870-17881 (2006).
76. Hulley, P., Hartikka, J. & Lubbert, H. Cyclic AMP promotes the survival of dopaminergic neurons in vitro and protects them from the toxic effects of MPP+. *Journal of neural transmission* **46**, 217-228 (1995).
77. Taylor, S.S., *et al.* PKA: a portrait of protein kinase dynamics. *Biochimica et biophysica acta* **1697**, 259-269 (2004).
78. Alto, N., Carlisle Michel, J.J., Dodge, K.L., Langeberg, L.K. & Scott, J.D. Intracellular targeting of protein kinases and phosphatases. *Diabetes* **51 Suppl 3**, S385-388 (2002).
79. Roche, K.W., O'Brien, R.J., Mammen, A.L., Bernhardt, J. & Huganir, R.L. Characterization of multiple phosphorylation sites on the AMPA receptor GluR1 subunit. *Neuron* **16**, 1179-1188 (1996).
80. Nguyen, P.V. & Woo, N.H. Regulation of hippocampal synaptic plasticity by cyclic AMP-dependent protein kinases. *Progress in neurobiology* **71**, 401-437 (2003).
81. Budovskaya, Y.V., Stephan, J.S., Deminoff, S.J. & Herman, P.K. An evolutionary proteomics approach identifies substrates of the cAMP-dependent protein kinase. *Proceedings of the National Academy of Sciences of the United States of America* **102**, 13933-13938 (2005).
82. Holen, I., Gordon, P.B., Stromhaug, P.E. & Seglen, P.O. Role of cAMP in the regulation of hepatocytic autophagy. *European journal of biochemistry / FEBS* **236**, 163-170 (1996).
83. Feliciello, A., Gottesman, M.E. & Avvedimento, E.V. cAMP-PKA signaling to the mitochondria: protein scaffolds, mRNA and phosphatases. *Cellular signalling* **17**, 279-287 (2005).
84. Mattson, M.P. Mitochondrial regulation of neuronal plasticity. *Neurochemical research* **32**, 707-715 (2007).
85. Narendra, D., Tanaka, A., Suen, D.F. & Youle, R.J. Parkin is recruited selectively to impaired mitochondria and promotes their autophagy. *The Journal of cell biology* **183**, 795-803 (2008).
86. Kuznetsov, S.A. & Gelfand, V.I. 18 kDa microtubule-associated protein: identification as a new light chain (LC-3) of microtubule-associated protein 1 (MAP-1). *FEBS letters* **212**, 145-148 (1987).
87. Weihofen, A., Ostaszewski, B., Minami, Y. & Selkoe, D.J. Pink1 Parkinson mutations, the Cdc37/Hsp90 chaperones and Parkin all influence the maturation or subcellular distribution of Pink1. *Human molecular genetics* **17**, 602-616 (2008).
88. Smith, W.W., *et al.* Leucine-rich repeat kinase 2 (LRRK2) interacts with parkin, and mutant LRRK2 induces neuronal degeneration. *Proceedings of the National Academy of Sciences of the United States of America* **102**, 18676-18681 (2005).
89. Ng, C.H., *et al.* Parkin protects against LRRK2 G2019S mutant-induced dopaminergic neurodegeneration in Drosophila. *J Neurosci* **29**, 11257-11262 (2009).
90. Helton, T.D., Otsuka, T., Lee, M.C., Mu, Y. & Ehlers, M.D. Pruning and loss of excitatory synapses by the parkin ubiquitin ligase. *Proceedings of the National Academy of Sciences of the United States of America* **105**, 19492-19497 (2008).

91. Cui, J., Yu, M., Niu, J., Yue, Z. & Xu, Z. Expression of Leucine-Rich Repeat Kinase 2 (LRRK2) Inhibits the Processing of uMtCK to Induce Cell Death in cell culture model system. *Bioscience reports* (2011).
92. Biskup, S.*, et al.* Localization of LRRK2 to membranous and vesicular structures in mammalian brain. *Annals of neurology* **60**, 557-569 (2006).
93. Li, Z., Okamoto, K., Hayashi, Y. & Sheng, M. The importance of dendritic mitochondria in the morphogenesis and plasticity of spines and synapses. *Cell* **119**, 873-887 (2004).
94. Wang, Q.J.*, et al.* Induction of autophagy in axonal dystrophy and degeneration. *J Neurosci* **26**, 8057-8068 (2006).
95. Kim, I. & Lemasters, J.J. Mitophagy selectively degrades individual damaged mitochondria after photoirradiation. *Antioxidants & redox signaling* **14**, 1919-1928 (2011).
96. Gallusser, A. & Kirchhausen, T. The beta 1 and beta 2 subunits of the AP complexes are the clathrin coat assembly components. *The EMBO journal* **12**, 5237-5244 (1993).
97. Kirchhausen, T. Three ways to make a vesicle. *Nature reviews* **1**, 187-198 (2000).
98. Ravikumar, B., Moreau, K., Jahreiss, L., Puri, C. & Rubinsztein, D.C. Plasma membrane contributes to the formation of pre-autophagosomal structures. *Nature cell biology* **12**, 747-757 (2010).
99. Fader, C.M. & Colombo, M.I. Autophagy and multivesicular bodies: two closely related partners. *Cell death and differentiation* **16**, 70-78 (2009).
100. Barbe, L.*, et al.* Toward a confocal subcellular atlas of the human proteome. *Mol Cell Proteomics* **7**, 499-508 (2008).
101. Sims, H.F.*, et al.* The molecular basis of pediatric long chain 3-hydroxyacyl-CoA dehydrogenase deficiency associated with maternal acute fatty liver of pregnancy. *Proceedings of the National Academy of Sciences of the United States of America* **92**, 841-845 (1995).
102. Huber, A., Bai, P., de Murcia, J.M. & de Murcia, G. PARP-1, PARP-2 and ATM in the DNA damage response: functional synergy in mouse development. *DNA repair* **3**, 1103-1108 (2004).
103. Tang, J.B.*, et al.* Bioenergetic metabolites regulate base excision repair-dependent cell death in response to DNA damage. *Mol Cancer Res* **8**, 67-79 (2010).
104. Banerjee, J. & Ghosh, S. Phosphorylation of rat brain mitochondrial voltage-dependent anion as a potential tool to control leakage of cytochrome c. *Journal of neurochemistry* **98**, 670-676 (2006).
105. Pediaditakis, P.*, et al.* Inhibition of the mitochondrial permeability transition by protein kinase A in rat liver mitochondria and hepatocytes. *The Biochemical journal* **431**, 411-421 (2010).
106. Papa, S.*, et al.* cAMP-dependent protein kinase regulates post-translational processing and expression of complex I subunits in mammalian cells. *Biochimica et biophysica acta* **1797**, 649-658 (2010).
107. Cribbs, J.T. & Strack, S. Reversible phosphorylation of Drp1 by cyclic AMP-dependent protein kinase and calcineurin regulates mitochondrial fission and cell death. *EMBO reports* **8**, 939-944 (2007).
108. Chang, C.R. & Blackstone, C. Cyclic AMP-dependent protein kinase phosphorylation of Drp1 regulates its GTPase activity and mitochondrial morphology. *The Journal of biological chemistry* **282**, 21583-21587 (2007).
109. Raman, I.M., Tong, G. & Jahr, C.E. Beta-adrenergic regulation of synaptic NMDA receptors by cAMP-dependent protein kinase. *Neuron* **16**, 415-421 (1996).

110. Petrovic, M.M., Vales, K., Putnikovic, B., Djulejic, V. & Mitrovic, D.M. Ryanodine receptors, voltage-gated calcium channels and their relationship with protein kinase A in the myocardium. *Physiological research / Academia Scientiarum Bohemoslovaca* **57**, 141-149 (2008).
111. Wicher, D. Peptidergic modulation of insect voltage-gated Ca(2+) currents: role of resting Ca(2+) current and protein kinases A and C. *Journal of neurophysiology* **86**, 2353-2362 (2001).
112. Reiken, S.*, et al.* PKA phosphorylation activates the calcium release channel (ryanodine receptor) in skeletal muscle: defective regulation in heart failure. *The Journal of cell biology* **160**, 919-928 (2003).
113. Hoddah, H., Marcantoni, A., Comunanza, V., Carabelli, V. & Carbone, E. L-type channel inhibition by CB1 cannabinoid receptors is mediated by PTX-sensitive G proteins and cAMP/PKA in GT1-7 hypothalamic neurons. *Cell calcium* **46**, 303-312 (2009).
114. Fawcett, J.P.*, et al.* Evidence that brain-derived neurotrophic factor from presynaptic nerve terminals regulates the phenotype of calbindin-containing neurons in the lateral septum. *J Neurosci* **20**, 274-282 (2000).
115. Palmieri, F. The mitochondrial transporter family (SLC25): physiological and pathological implications. *Pflugers Arch* **447**, 689-709 (2004).
116. Tan, W. & Colombini, M. VDAC closure increases calcium ion flux. *Biochimica et biophysica acta* **1768**, 2510-2515 (2007).
117. Abou-Sleiman, P.M.*, et al.* A heterozygous effect for PINK1 mutations in Parkinson's disease? *Annals of neurology* **60**, 414-419 (2006).
118. Khan, N.L.*, et al.* Clinical and subclinical dopaminergic dysfunction in PARK6-linked parkinsonism: an 18F-dopa PET study. *Annals of neurology* **52**, 849-853 (2002).
119. Zhou, H.*, et al.* Silencing of the Pink1 gene expression by conditional RNAi does not induce dopaminergic neuron death in mice. *International journal of biological sciences* **3**, 242-250 (2007).